Physically based remote sensing methods and illustrating the challenges of monitoring vegetation: new angles on an old problem

Jan Pisek, Tiit Nilson, Andres Kuusk
Tartu Observatory, Toravere, Estonia

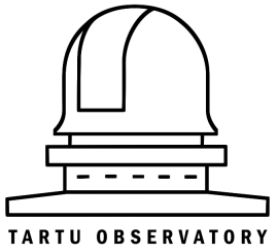

IKI. November 15, 2010. Moscow,Russia

PhD., University of Toronto (2005-2009)
Prof. Jing Ming Chen's group

Tartu Observatory (2009-present)
Tiit Nilson, Andres Kuusk

Juhan Ross (1925-2002)
"The Radiation Regime and Architecture of Plant Stands" by Gidrometeoizdat, Leningrad, 1975 in Russian and by Dr. W. Junk Publishers, The Hague, 1981, serves as a handbook in this field

Physically based remote sensing methods and illustrating the challenges of monitoring vegetation: new angles on an old problem

Jan Pisek, Tiit Nilson, Andres Kuusk
Tartu Observatory, Toravere, Estonia

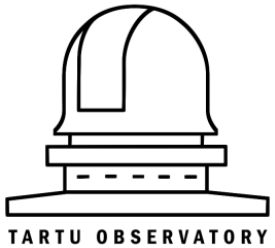

IKI. November 15, 2010. Moscow,Russia

Physically based remote sensing

- A set of methods which apply reflectance models to interpret the spectral-directional signatures obtained from air-borne or satellite-borne images

Reflectance models

- Used to describe the upwelling radiation field of an object such as a forest or an agricultural field
- The reflectance spectrum of an object (e.g. forest stand) may, if interpreted correctly, be used to identify it and to quantify its structural, physical and chemical properties

Biophysical variables

-Defined as state variables that directly control the process of radiative transfer in vegetation canopies (e.g. the amount of photosynthesizing leaf area in vegetation)

Physical Models in Remote Sensing

- Quantitative remote sensing has become operational
- Typically, computer packages are applied, you see the input and output, only. No idea what is 'inside', it works like a black box

Why do we need physical reflectance models?

- To establish quantitative relations between reflected signal and various input parameters
- To understand how the reflected signal is formed
- Finding out the most important driving factors determining the spectral, angular, temporal and spatial behaviour of reflectance
- Making various numerical experiments including those 'pure' experiments that never could occur in nature
- Interpretation and normalization of measurement results
- To derive methods of inversion for important vegetation parameters
- Deriving algorithms for producing albedo, absorbed PAR, etc. of ground surface from directional measurements

Vegetation canopy reflectance

- What controls the spectral properties of individual leaves?
- Surface roughness
- Refractive index of cuticle
- Composition, amount and distribution of pigments
- Internal leaf structure
- Distribution of water
- PROSPECT (Jacquemond and Baret, 1990) just three input variables: leaf chlorophyll content, leaf water content, and a leaf structure parameter to predict leaf reflectance in 400- to 2500- nm range

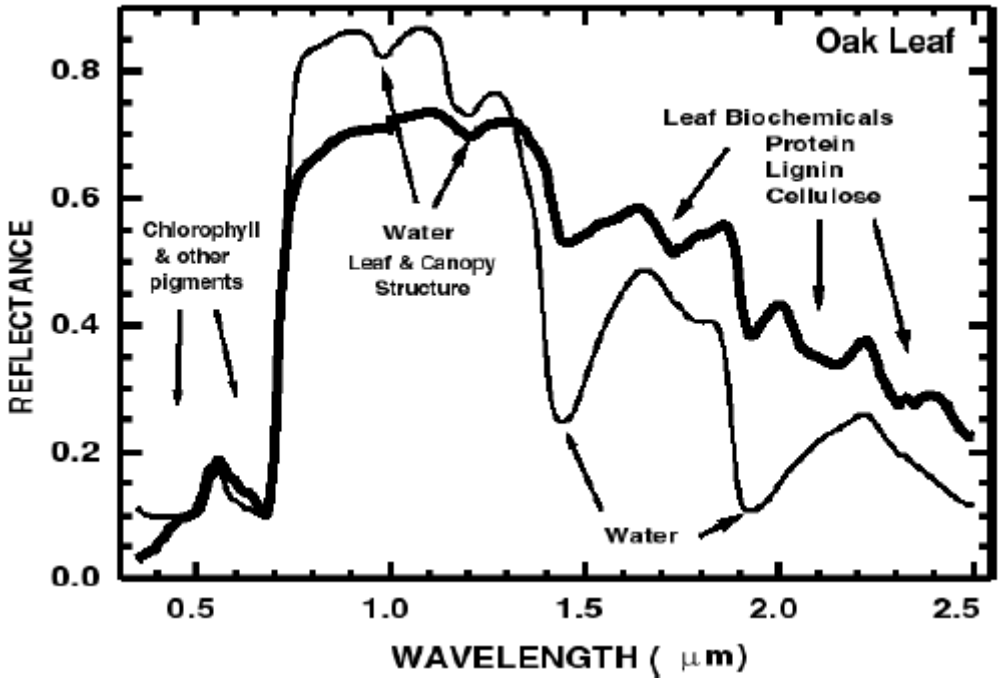

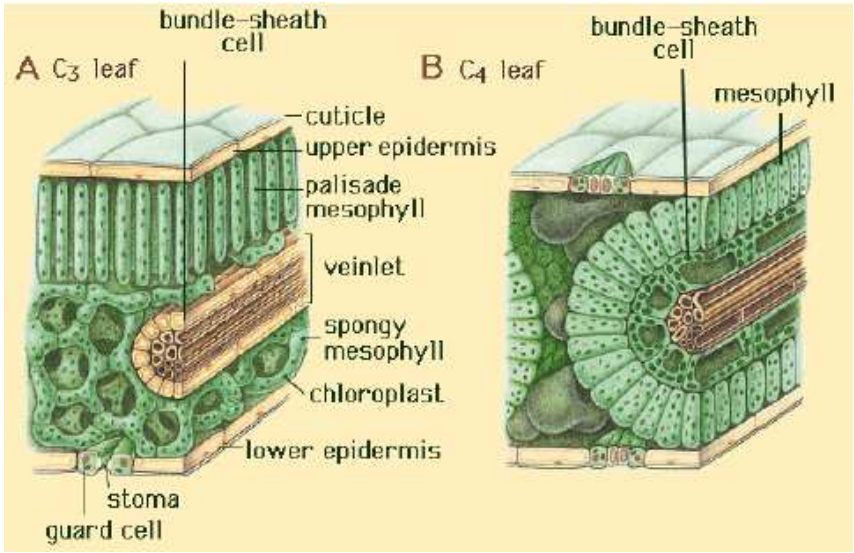

Image source: D. Baldocchi, UC Berkeley

Leaf area index

- one half of the total all-sided green leaf area per unit horizontal ground surface area (Chen and Black, 1992)

LAI = 2.25

LAI = 4.75

- In general a negative relationship between LAI and visible reflectance and a positive relationship with NIR reflectance

Soil reflectance

- Wavelength-dependant and must be defined for each waveband that is to be modeled
- Detemined by a wide range of soil properties (moisture content, mineral composition, organic matter content, roughness
- Vegetation canopy reflectance increases as soil reflectance increases
- The effect most important for sparse canopies (low LAI) where a large amount of background is visible

Leaf angle distribution

- Leaves in vegetation canopies rarely horizontal but are inclined at a range of angles described by the leaf angle distribution (LAD) function
- Quantifies the frequency of leaves at a given inclination angle
- A number of idealized LAD have been defined to describe the structure of vegetation canopies

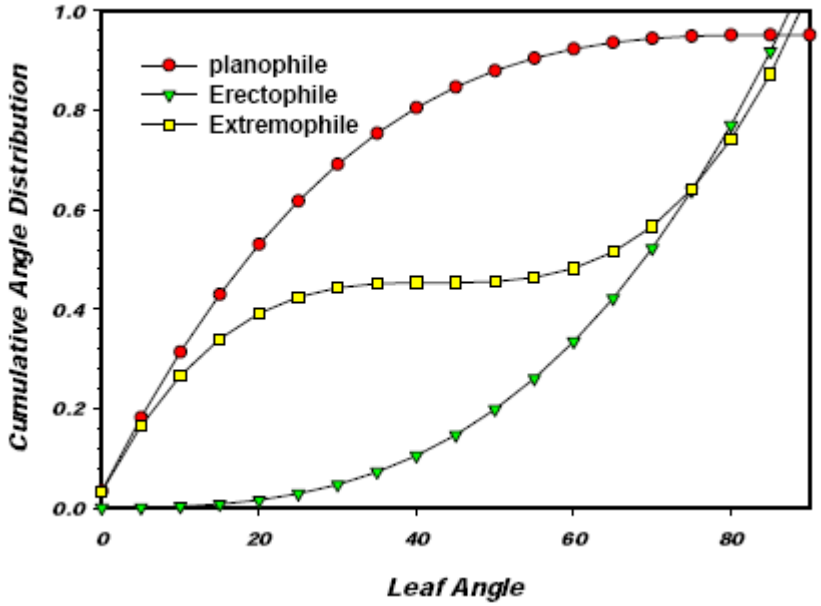

Image source: D. Baldocchi, UC Berkeley

Spatial organization of leaves in the canopy - foliage clumping (Ω)

- quantifies the degree of the deviation of foliage spatial distribution from the random case (Nilson, 1971)

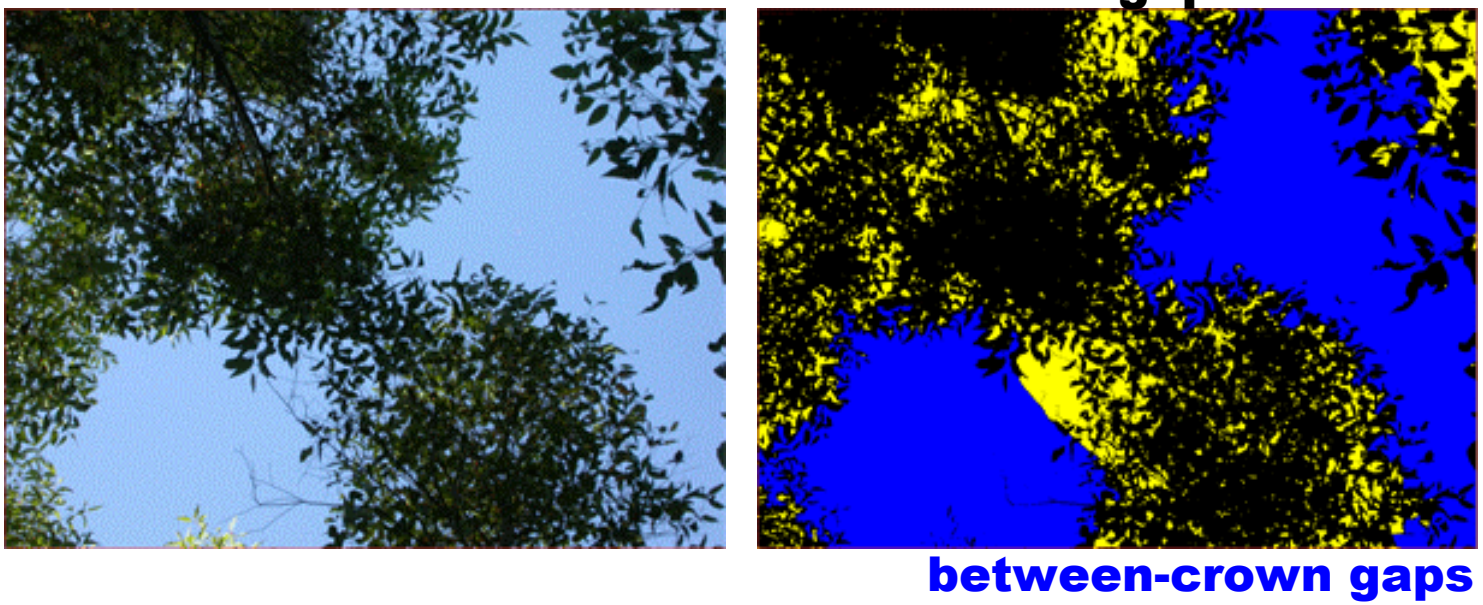

- affects the gap fraction for the same LAI
- affects both radiation interception and distribution within the canopy => photosynthesis and evaporation

Images property of Regent Instruments, Quebec, Canada

Illumination and view geometry

- Reflectance of a vegetation canopy generally non-Lambertian
- Dependent on the angle at which it is illuminated by the Sun and viewed by the remote sensor
- Bi-directional reflectance distribution function (BRDF)

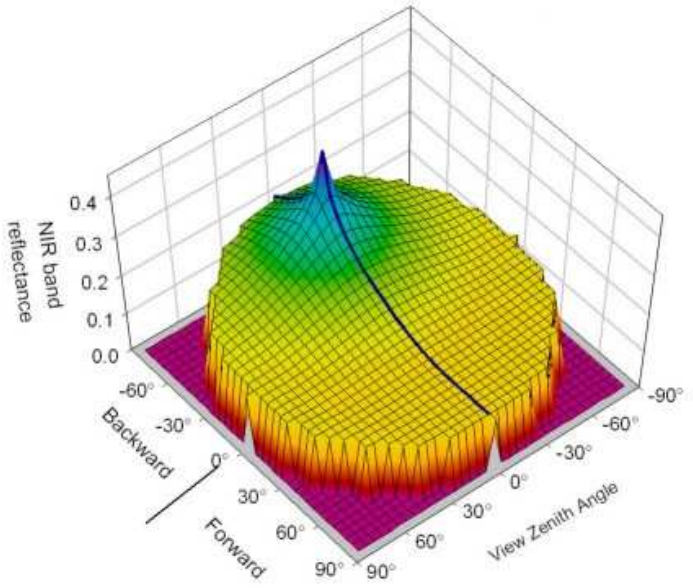

Hotspot Image source: Andres Kuusk

Radiative transfer in turbid media

- Developed well enough for solving problems in astrophysics, nuclear physics and atmospheric physics
- Marchuk 1961 on the process of neutron transfer
- **Marchuk GI, 1961. Methods of calculation of nuclear reactors. Atomizdat, Moscow (in Russian)**
- Chandrasekhar 1950 and Sobolev 1963 on astrophysical problems
- **Sobolev VV, 1963. A treatise of radiative transfer. Nostrand (original publ. 1956)**
- Vladimirov 1961 for a mathematical description of transport theory
- **Vladimirov VV, 1963. Mathematical problems in the one-velocity theory of particle transport. AECL-1661. (original publ. 1961)**
- A formal way of developing RT theory in leaf canopies using the analogy of a turbid layer can be found in Shifrin (1953)
- **Shifrin KS (1953) Concerning the theory of albedo. Trans Main Geophys Obs 39, 101:244-257 (in Russian)**
- Further developed by Ross and co. (1981) at Tartu Observatory

Turbid medium approach

- Introduced to modeling the radiation regime inside vegetation by Ross (1981)
- Based on some approximate solution of the RT equation
- Kubelka-Munk four flux approximation (1931) – two stream (up and down)
- Canopy RT models based on Kubelka-Munk theory: coefficients of K-M equations are in some way related to the vegetation parameters
- Turbid medium models assume that the canopy may be represented by small absorbing and scattering elements, with known optical properties, distributed randomly in horizontal layers and with a known angular distribution (Goel, 1988)
- SAIL (Verhoef, 1984) the best known for a homogeneous canopy reflectance model – reasonably accurate for relatively homogeneous canopies

3D reflectance models

- Useful for highly structured scenes where two-stream model not good
- Canopy divided into cells
- Method based on the calculation of radiation intensities in discretized directions
- In each iteration, the contribution of radiation scattered to every discrete direction from all other directions is calculated for each canopy cell using a pre-calculated scattering matrix until the intensities converge to a solution
- the 3D radiative transfer computations used to predict forest canopy reflectance not only computationally intensive, but also require much detailed information on forest structure than what is commonly available.

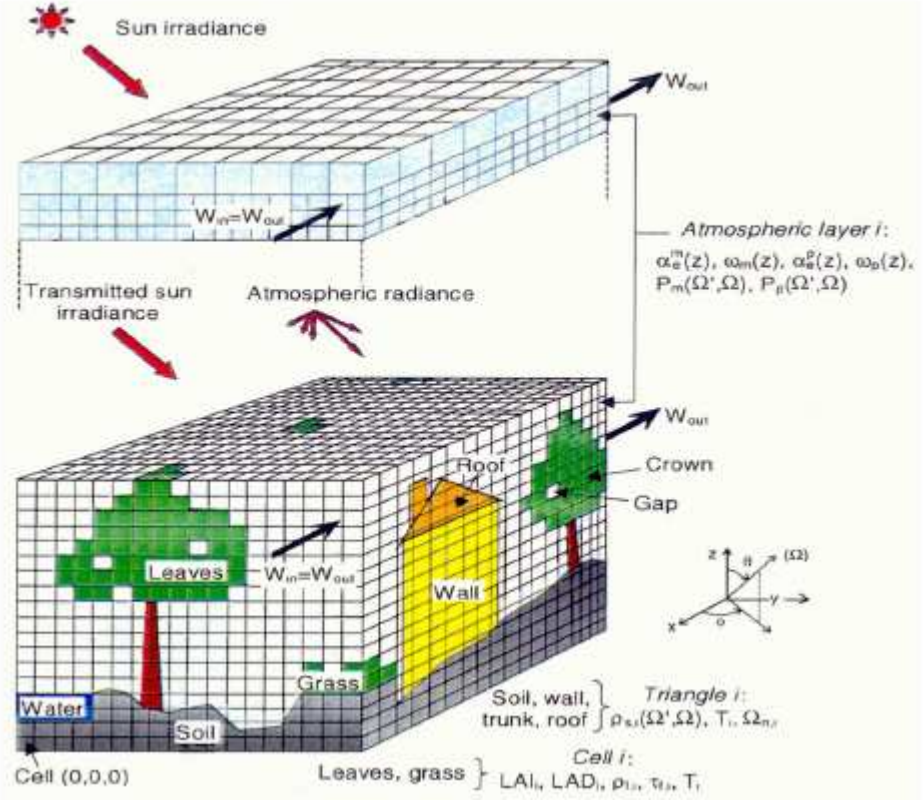

GastelluEtchegorry et al., 2001

Monte Carlo approach

- Radiation field above plant canopy composed of small contributions by individual photons
- The angular and spatial variation in the intensity of reflected radiation can be viewed as a distribution function describing the possible exit directions
- Monte Carlo (or ray tracing methods) based on random sampling of this distribution
- Overview of the Monte Carlo modeling approach in Disney et al. (2000)

Geometric-optical (GO)/hybrid models

- Often a compromise among the level of detail, robustness and accuracy

- Represent canopy as an aggregation of geometric tree crown envelopes whose locations are described by a statistical distribution

-the stand parameters correspond more closely to what can actually be measured in a forest: crown dimensions, canopy closure, etc.

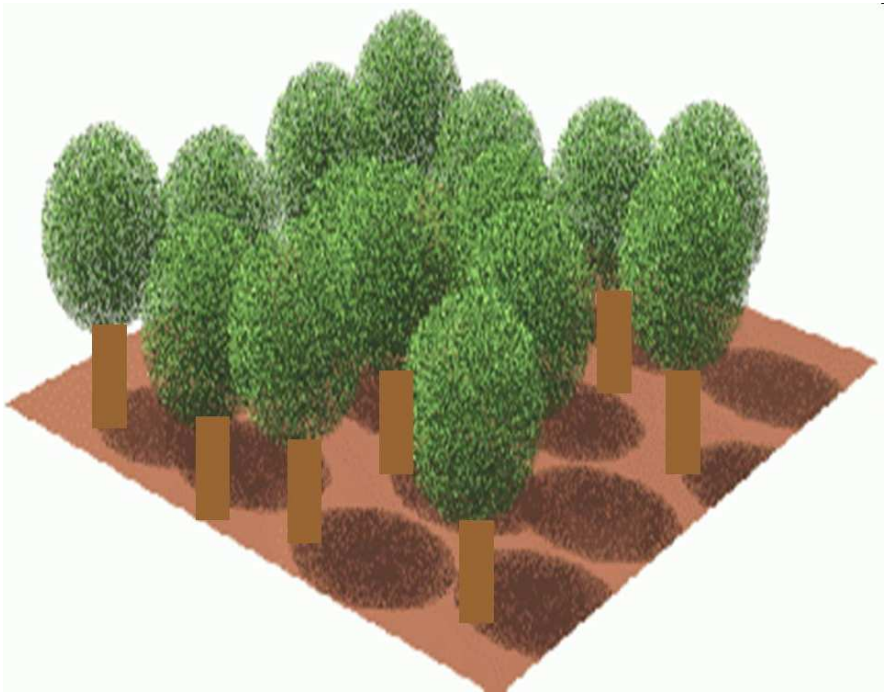

Inversion of a forest reflectance model

- to obtain biophysical variables from remote sensing data.
- The task of interpreting the spectral-directional signature of a forest can be reduced to matching the measured reflectance signal to a known simulated signal
- Inversion ill-posed problem (many parameterizations of a reflectance model can correspond to the same measured reflectance)
-Iterative optimization may be used: the values of the unknown parameters are slightly modified between consecutive model runs until the model-predicted reflectance spectrum fits the observed closely enough.

-In operational environments
=> a look-up table is usually computationally more efficient if it is used repeatedly (e.g. Knyazikhin et al., 1998a)
- theoretically, neural networks should be the fastest inversion method (Liang, 2007)

How to pick up a model?

- Amount of required computer resources, manpower and time
- Object under investigation
- If canopy reflectance calculations from only a small contribution to a larger problem with many variables and uncertainties, simpler model is justified
- Amount of a priori knowledge

What is RAMI about ?

RAdiation transfer Model Intercomparison (RAMI) is an on-going mechanism to benchmark radiation transfer (RT) models used to simulate the transfer of radiation at or near the Earth's terrestrial surface, i.e. in plant canopies and over soil surfaces

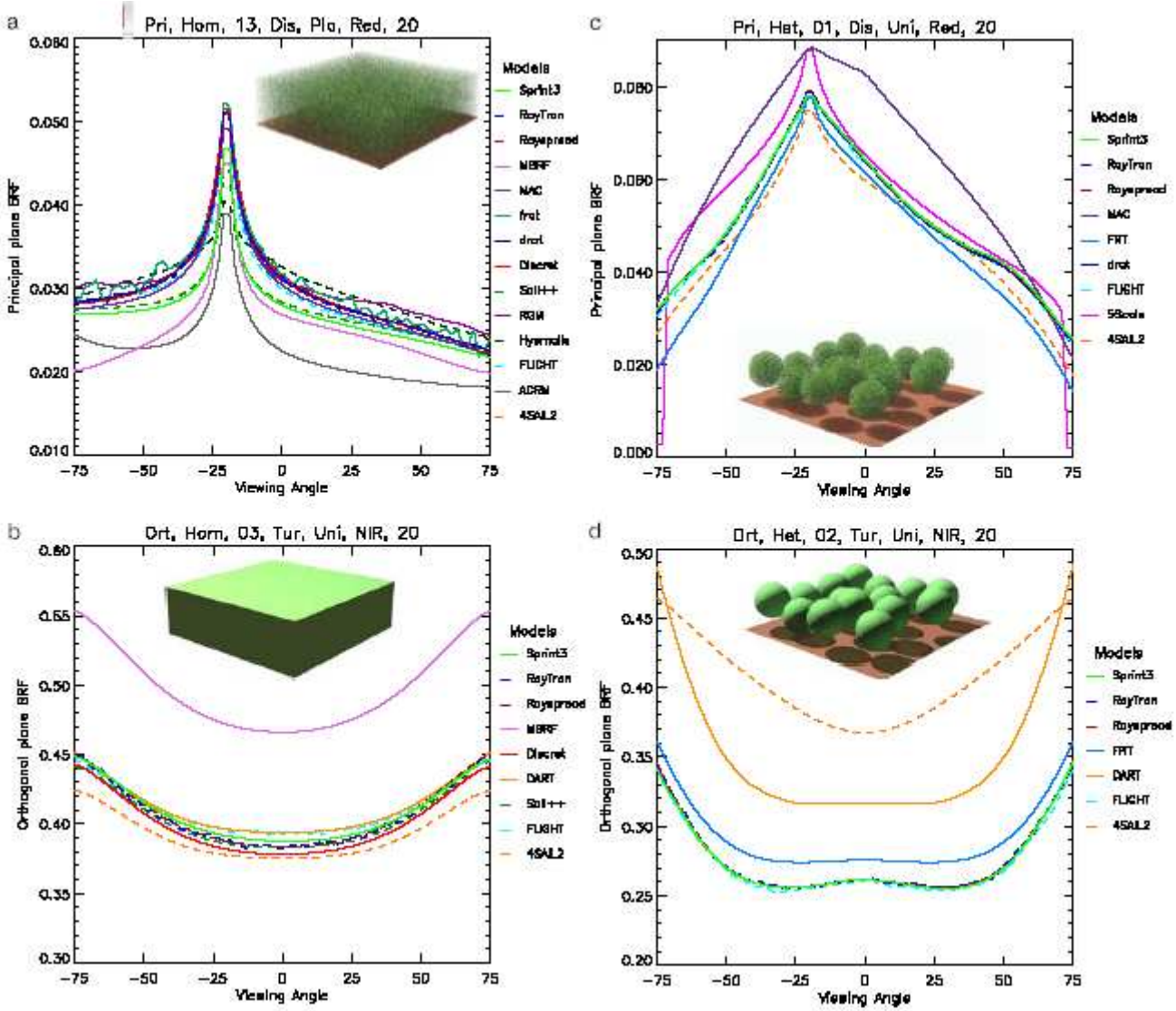

Widlowski et al. (2007, JGR)

http://rami-benchmark.jrc.ec.europa.eu/HTML/

Most common remotely sensed biophysical variables of vegetation

LAI (leaf area index)

Fraction of canopy cover (fCover)

- LAI and fCover geometrical variables related to canopy gap fraction (Nilson, 1977)
- Canopy gap fraction is in fact determined by LAI and its spatial distribution and leaf inclination distribution

Fraction of photosynthetically active radiation absorbed by Vegetation (fPAR)

- fPAR outcome of radiative transfer in vegetation (opposite of reflectance from vegetation)
- There are other biophysical variables which are not geometric,but influence the spectral properties of scattering elements (i.e. chlorophyll content of green leaves)
- However, there is evidence that no clear distinction between foliar biochemistry and LAI can be made in practical remote sensing (Yoder and Pettigrew-Crosby, 1995)

How biophysical variables estimated from remotely sensed data

- Empirical models calibrated with in-situ measurements
- Retrieval based on statistical relationships modeled between the concurrently acquired in situ and surface reflectance data, which are typically expressed in the form of vegetation index (VI)
- VIs various combinations of signal values in multispectral bands designed to maximize sensitivity to vegetation characteristics, while minimizing the sensitivity to atmosphere, background, view and solar angles
- VIs represent composite properties of the different biophysical variables
- Moderately useful in predicting individual canopy properties
- But site, sensor and time specific

Several ways to use reflectance models

- Simplest approach is to use model simulations to calibrate the relationships between model parameters and VIs
- VIs do not fully utilize the information of spectral-directional signatures
- The more advanced models include:
    - Iterative optimization algorithms (too demanding at a global scale)
    - LUTs and advanced statistical methods (neural networks – for faster operational inversion)
    - LUT used to search for a set of reflectance values most similar, goodness of fit measured with a merit function
    - Accurate inversion may require large LUT dimensions; may slow down the search process (MODIS)
    - In neural networks, a database of model simulations is used only once when calibrating the networks (MERIS, CYCLOPES)

Ecological variables of current interest in remote sensing

LAI (leaf area index)

- one half of the total leaf surface area per unit ground surface area projected on the local horizontal datum (Chen and Black, 1992; Morisette et al., 2006)

LAI = 2.25

LAI = 4.75

- key characteristic of interest in forest ecosystems because the green leaves control the processes driving the exchange of matter and energy

LAI global datasets

- **NOAA/AVHRR** Sellers et al. 1996; Los et al. 2000; Myneni et al., 1997; Buermann et al., 2002
- **ECOCLIMAP** Masson et al., 2003
- **SPOT-VEGETATION** Baret et al., 2007; Deng et al., 2006
- **TERRA/MODIS** Yang et al., 2006
- **ADEOS/POLDER** Roujean and Lacaze, 2002
- **ENVISAT/MERIS** Bacour et al., 2006
- **TERRA/MISR** Knyazikhin et al., 1998; Hu et al., 2003
- **MSG/SEVIRI** (http://landsaf.meteo.pt)

CYCLOPES LAI (Baret et al., 2007, RSE)

- Algorithm inputs atm. corrected red, NIR, SWIR reflectances from SPOT/VEGETATION normalized to a standard view-illumination geometry
- Cloud or snow cover observation removed
- Normalization performed by inversion of a reflectance model (Roujean and Lacaze, 2002) over data acquired during a moving compositing period of 30 days displaced by 10-day shifts
- LAI estimated using a neural network trained from 1-D radiative transfer SAIL model simulations

MODIS LAI (Knyazikhin et al., 1998)

- The main algorithm based on LUTs simulated from a 3D radiative transfer model (Knyazikhin et al., 1998)
- MODIS red and NIR atmospherically corrected reflectances and corresponding illumination-view geometry as inputs
- Algorithm output is the mean LAI computed over the set of acceptable LUT elements for which simulated and measured MODIS surface reflectances differ within specified levels of model and surface uncertainties
- If main algorithm fails, back up LAI-NDVI algorithm
- Parameters of both main and back-up algorithm defined for 8 vegetation types (MODIS land cover map used)

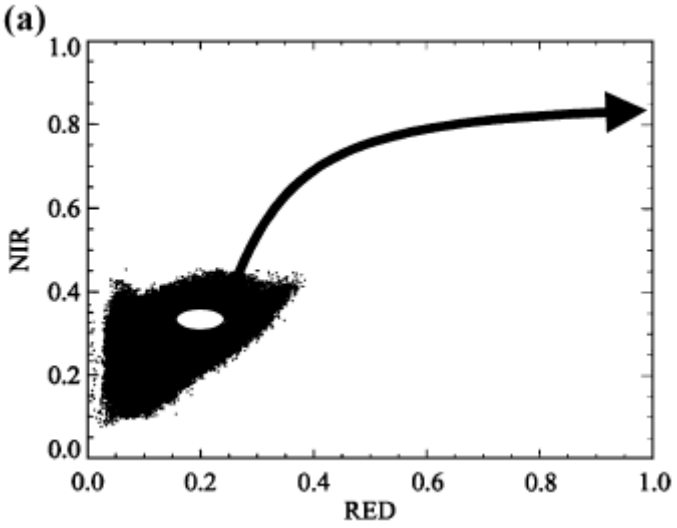

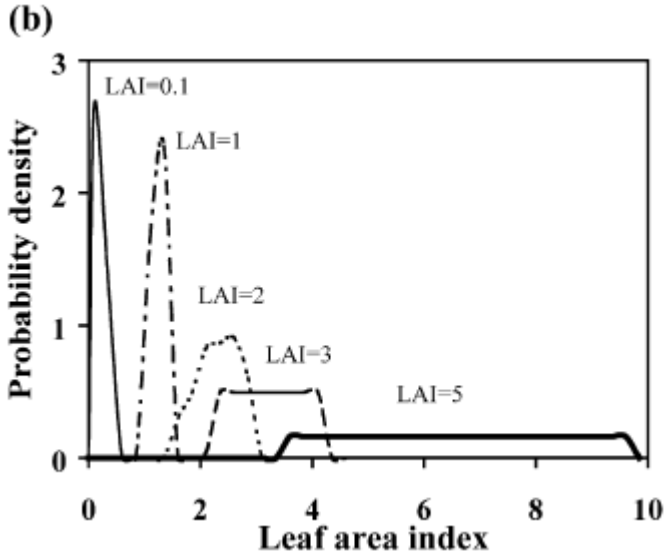

Myneni et al., 2002, RSE

UofT Global LAI product – algorithm for GLOBCARBON

- Global coverage in 1 km spatial resolution
- Global maps produced with a time-step of 10 days

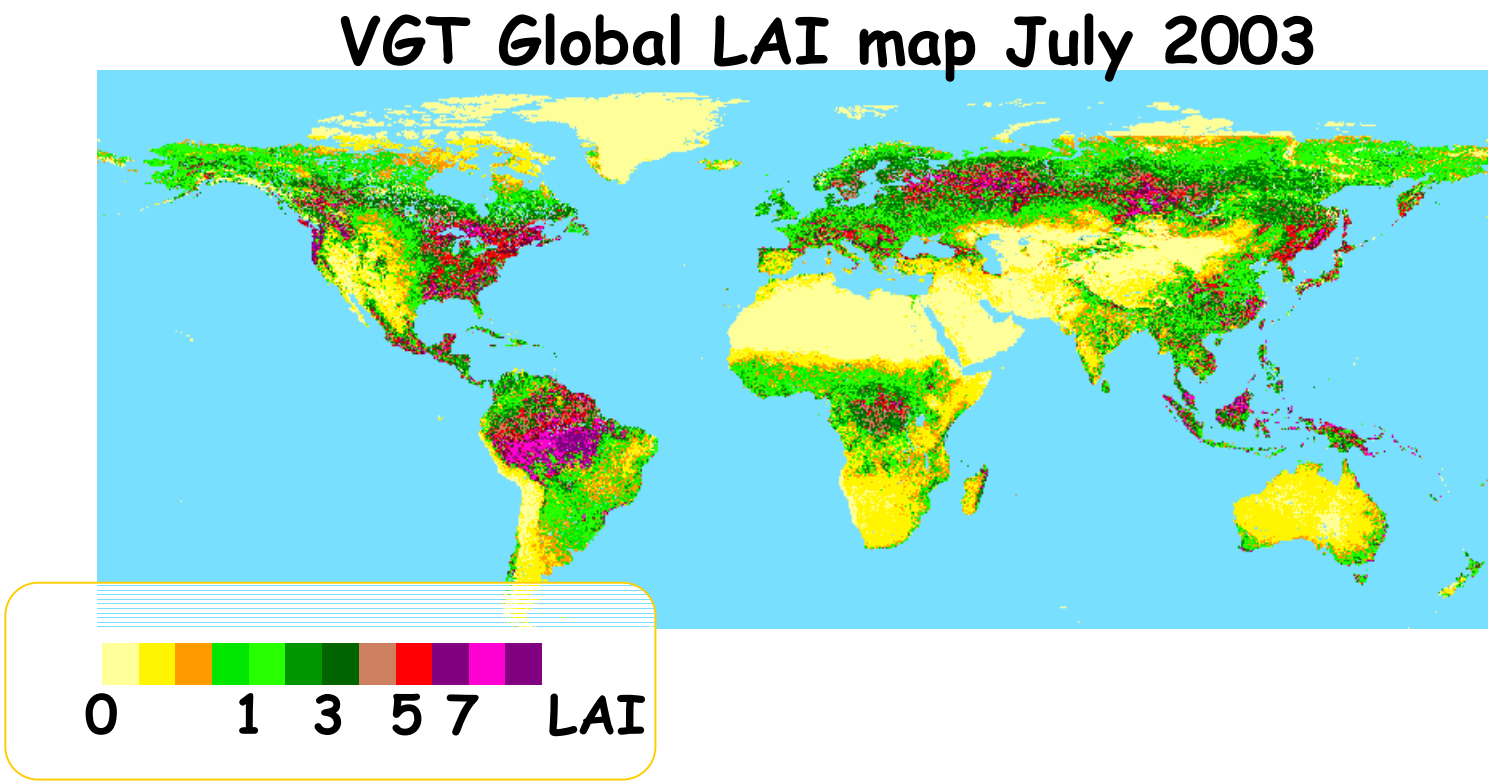

Deng et al., 2006, IEEE; Pisek and Chen, 2007, RSE

GO-RT model Four Scale (Chen and Leblanc, 1997)

- In forest canopies, the solar radiation is interacting with the foliage at four different scales: within groups of trees, within individual crowns, within branches, and within shoots.

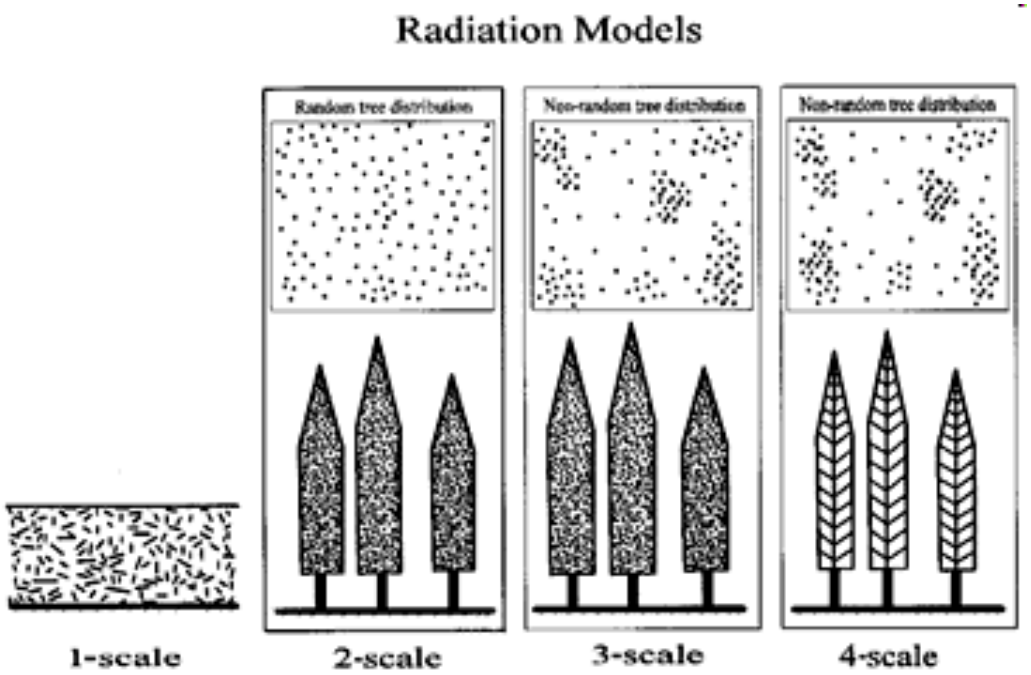

Chen and Leblanc, 1997, IEEE

Four Scale inputs

- site parameters (model domain size, LAI, tree density, tree grouping index, and SZA)
- tree architectural parameters (crown radius and height, apex angle, needle-to-shoot ratio, and typical leaf or shoot)
- spectral reflectivities of the foliage and the background in the various bands

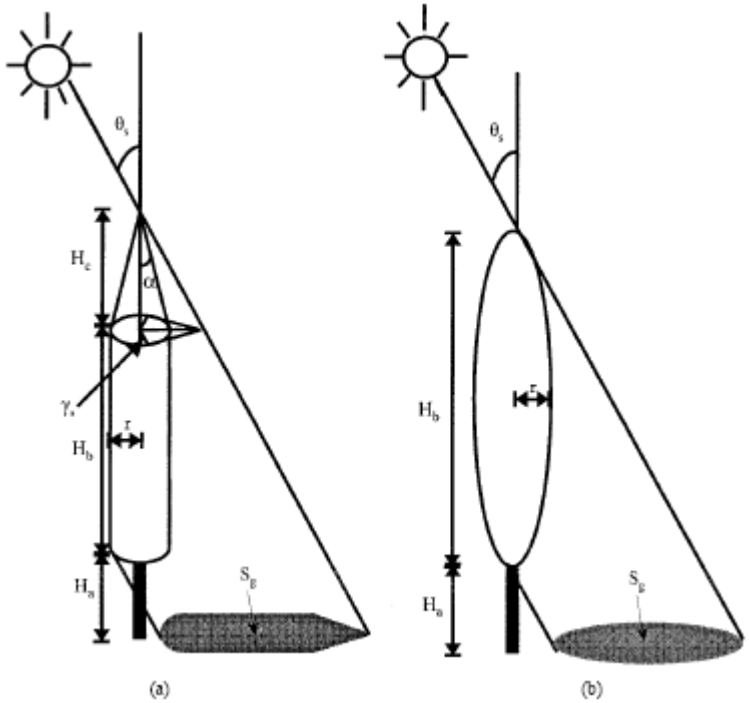

Leblanc and Chen, 1999, IEEE

Principles of Four Scale

1. The non-random spatial distribution of trees is simulated using the Neyman type A distribution (Neyman, 1939) that creates patches of a forest stand. The model simulates tree crowns as discrete geometrical objects: cone and cylinder for conifers, spheroid for deciduous species. The size of the crowns decreases when the trees are found in large clusters, and the tree locations are also subject to the repulsion effects to better represent the competition for light.

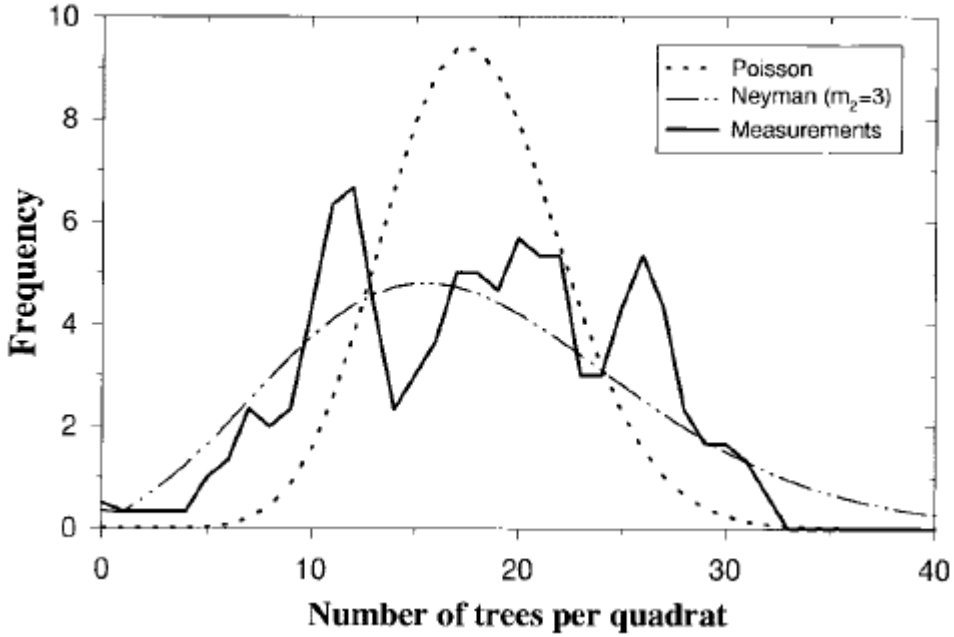

Chen and Leblanc, 1997, IEEE

Principles of Four Scale

2. Inside the crowns, a branch architecture defined by a single inclination angle is included to improve the calculation of light penetration from the geometric-optical model of Li and Strahler (1992) with the assumption of random leaf distribution inside tree crowns. A branch is in turn composed of foliage elements (individual leaves in deciduous and shoots in conifer canopies) with a given angle distribution pattern.

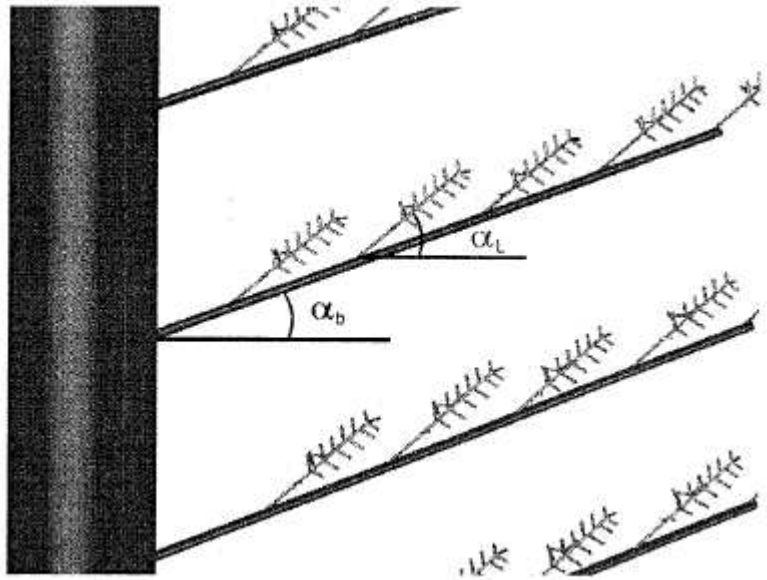

Leblanc and Chen, 1999, IEEE

Principles of Four Scale

3 The hotspot, where the view zenith and solar zenith angles coincide, is computed both on the ground and for the foliage with gap size distributions between and inside the crowns, respectively.

4. The crown is treated as a complex medium where shadowed foliage can be observed on the sunlit side, and sunlit foliage can be seen from the shaded side.

5. A multiple scattering scheme, based on view factors, is used to compute the amount of light reaching the shaded foliage and background.

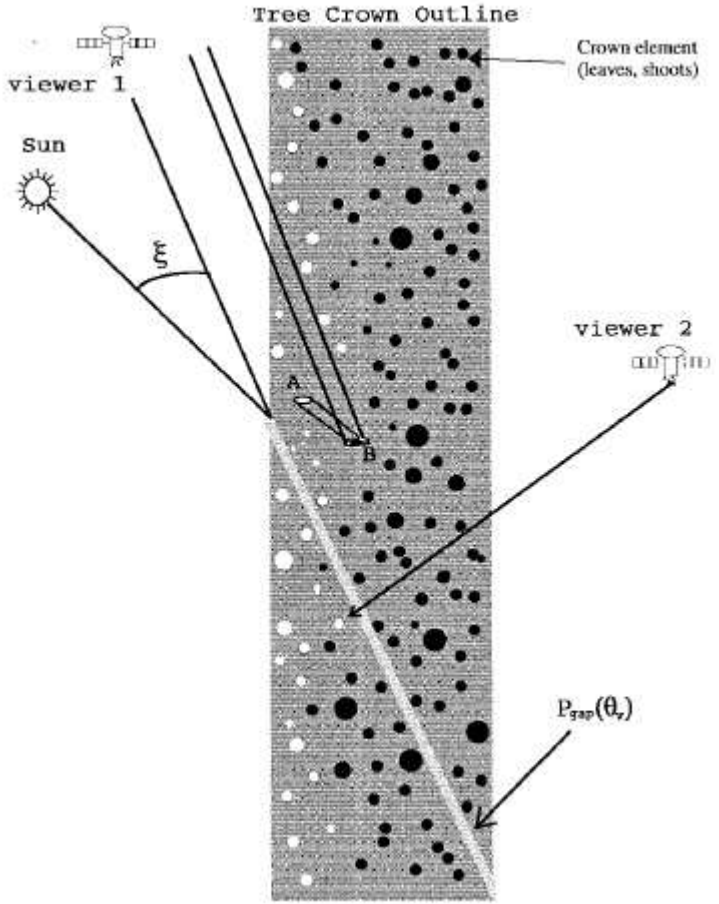

Chen and Leblanc, 1997, IEEE

Simulations of the LAI relationships with 4-Scale

- Four-Scale is used to simulate BRDF shapes and relationships between BRDF and LAI for each of the major cover types using a large combination of Four-Scale input parameters

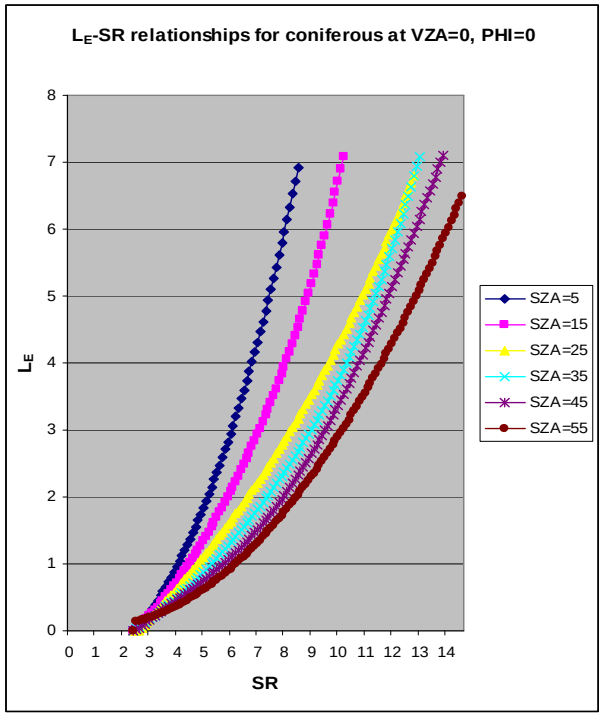

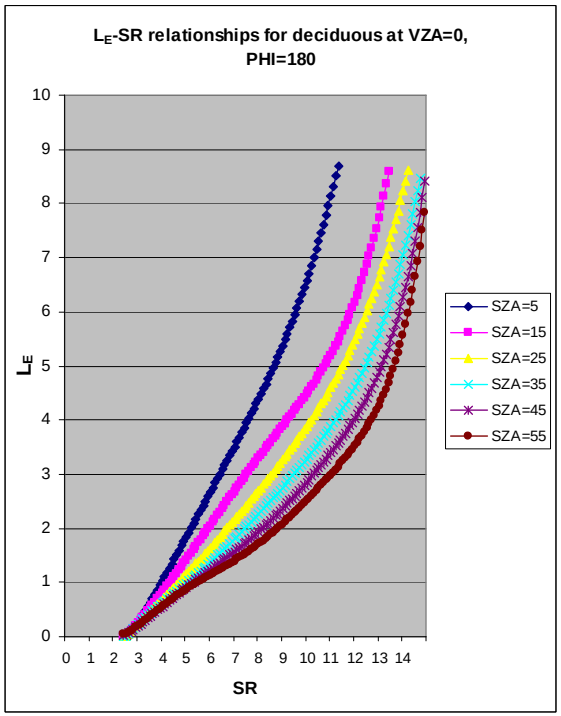

- these simulated results are processed into BRDF kernels using a curve-fitting technique
- Chebyshev polynomials of the second kind used since they are both accurate and easily implemented

Pafnuty Chebyshev (1821-1893)

Deng et al., 2006, IEEE

Specifics of the algorithm

- **BRDF effects are incorporated into LAI algorithms**

$$L = f_{\mathrm{L\_SR}}\left(\mathrm{SR} \cdot f_{\mathrm{BRDF}}\left(\theta_v, \theta_s, \phi, a_1(L), a_2(L)\right)\right)$$

$$L = f_{\mathrm{L\_RSR}}\left(\mathrm{SR} \cdot f_{\mathrm{BRDF}}(\theta_v, \theta_s, \phi, a_1(L), a_2(L)) \cdot \left(1 - \frac{\rho_{\mathrm{SWIR}} \cdot f_{\mathrm{SWIR\_BRDF}}(\theta_v, \theta_s, \phi, a_1(L), a_2(L)) - \rho_{\mathrm{SWIR\,min}}}{\rho_{\mathrm{SWIR\,max}} - \rho_{\mathrm{SWIR\,min}}}\right)\right)$$

- **Get precursor LAI, where** $f\mathrm{BRDF}(\theta vi, \theta si, \phi i) = 1$,
- **Get BRDF kernels with the precursor LAI**
- **Obtain BRDF modification functions**
- **Recalculate LAI from the BRDF kernels and VIs**

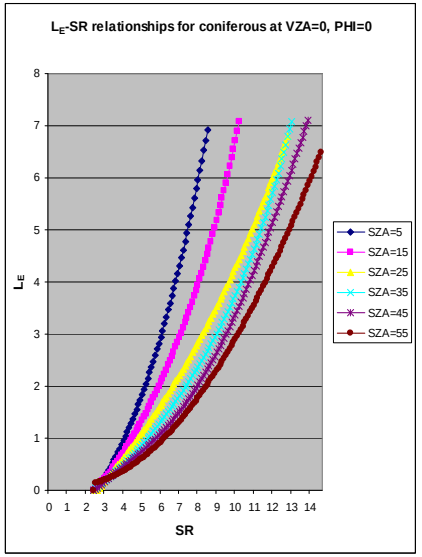

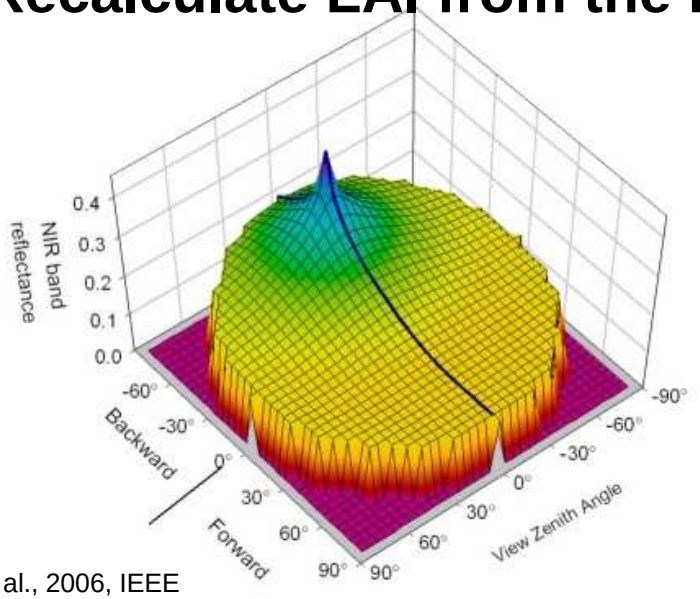

Deng et al., 2006, IEEE

Procedure to calculate LAI

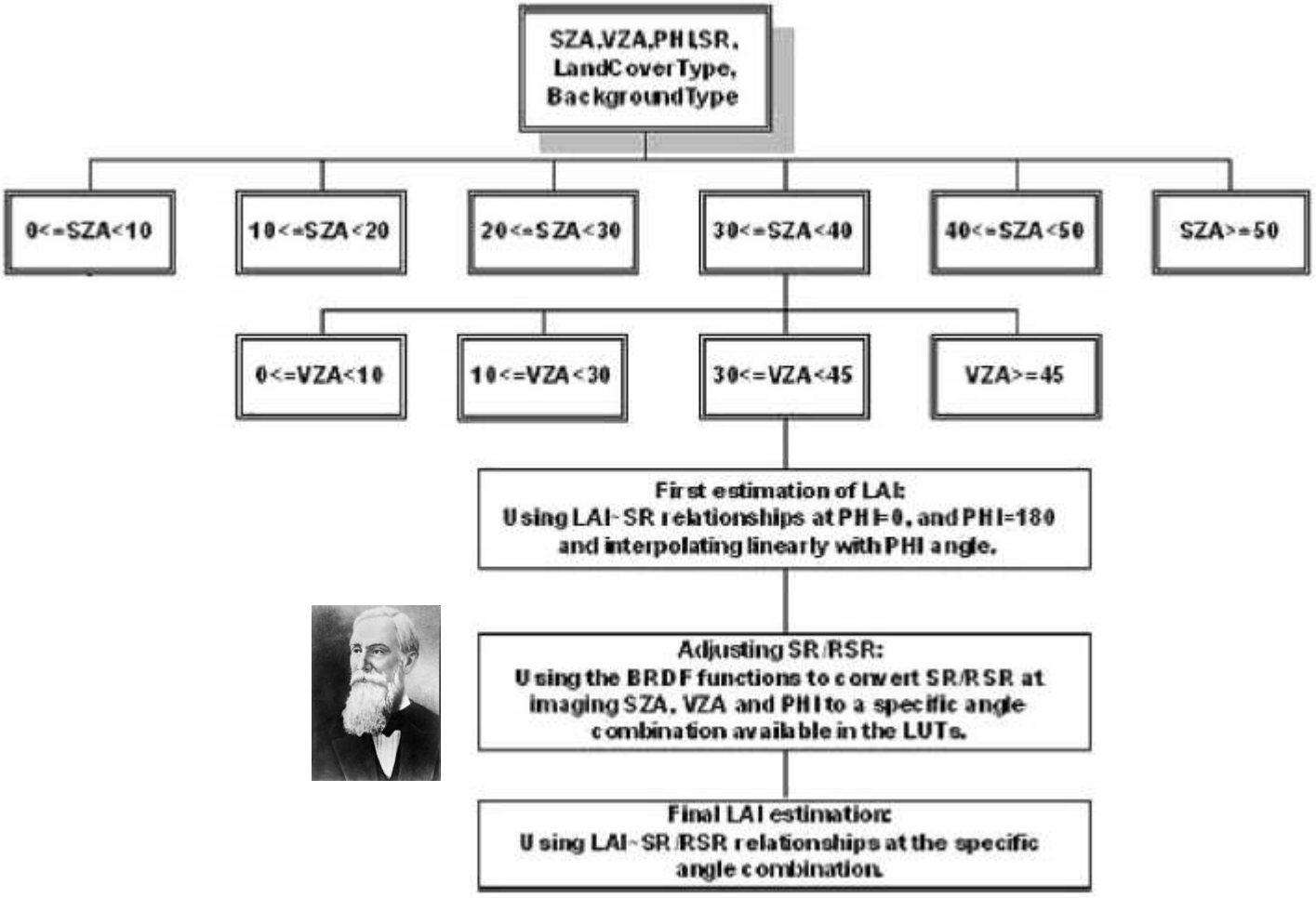

Deng et al., 2006, IEEE

Flow of the LAI model

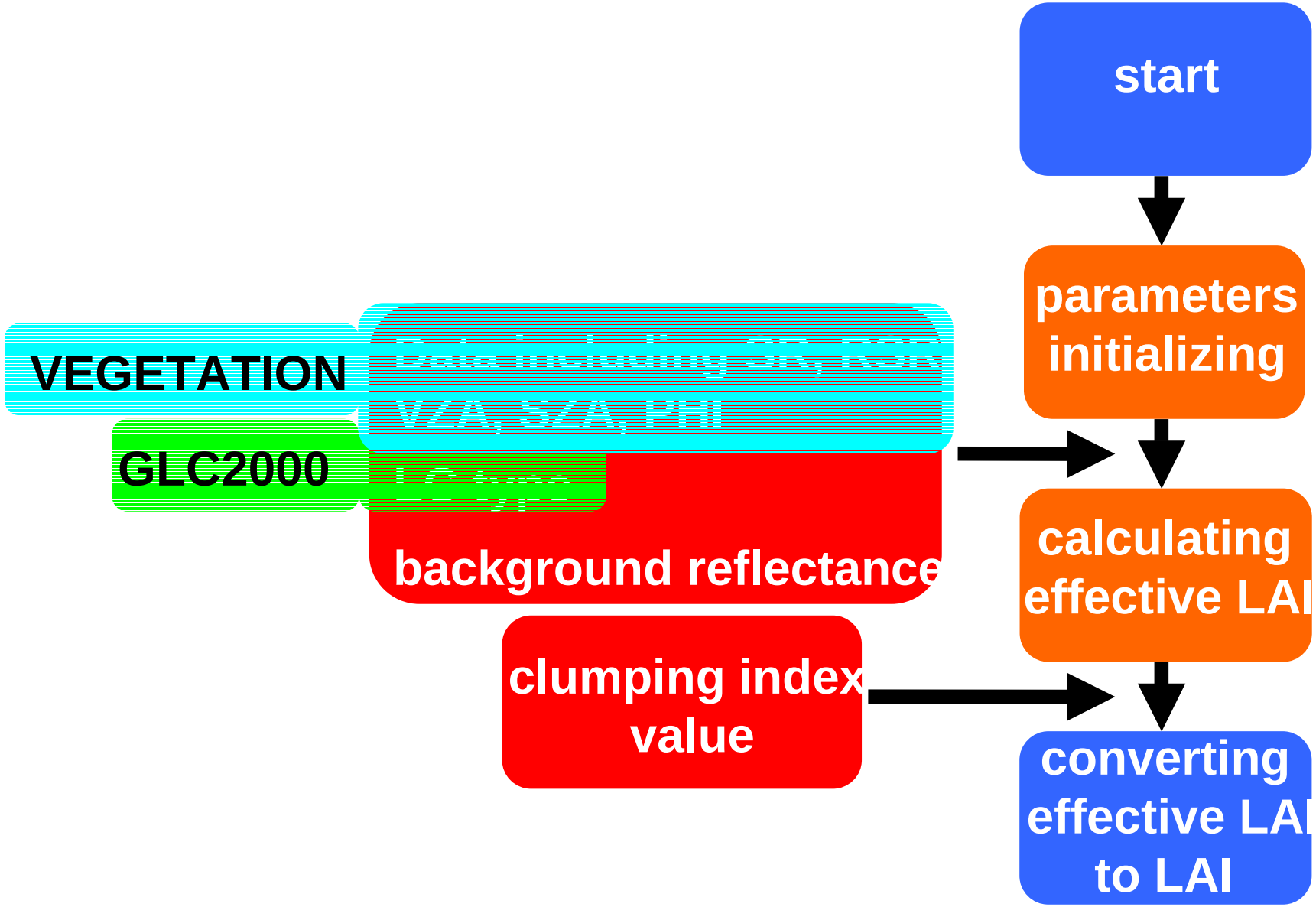

Deng et al., 2006, IEEE

Problems

- Inversion of canopy variables characteristically an ill-posed problem
- All types of pre/post processing
- Dependence on land cover types – sensitivity of classification errors
- LAI retrieval unstable – small variation in reflectance can result in a large change in LAI, particularly when the reflectance signal saturates (Knyazikhin et al. 1998)
- Intercomparison of LAI products has shown considerable differences between the datasets, particularly over forested areas
- One major source of uncertainty is the different representation of the grouping of foliage at different scales
- Understory LAI and woody material are considered with diverse methods
- Substantial land cover dependent differences have also been noted among global fAPAR datasets over northern Eurasia (McCallum et al., 2010)
- Snow effects

Validation A: TM Validation Sites

- 8 validation sites from Canada

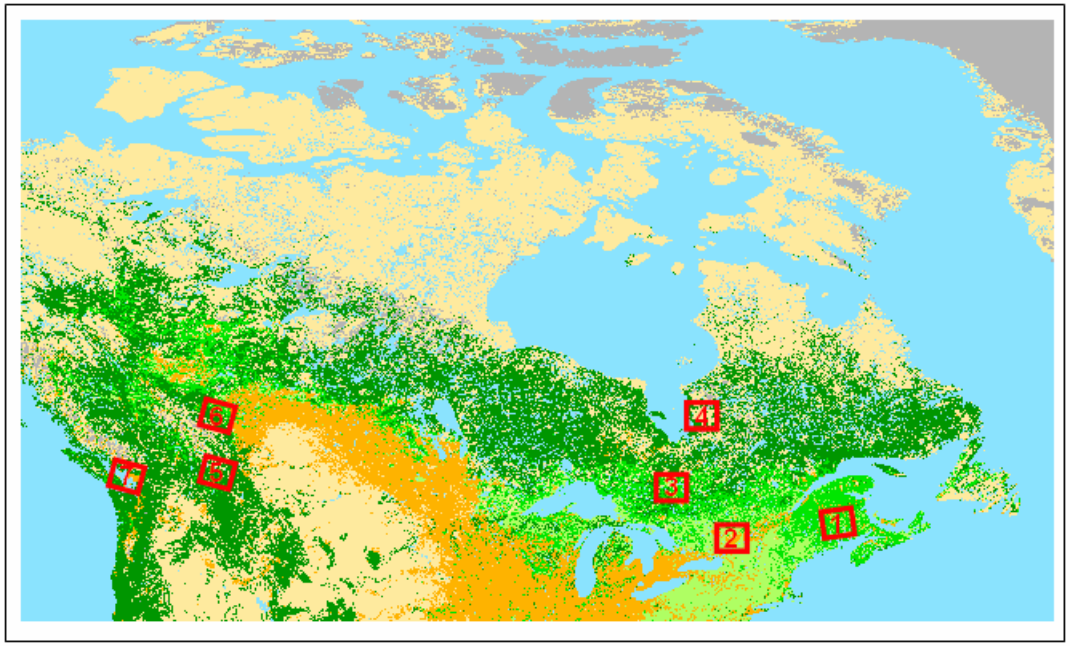

Pisek et al., 2007, CJRS

Possible sources of errors

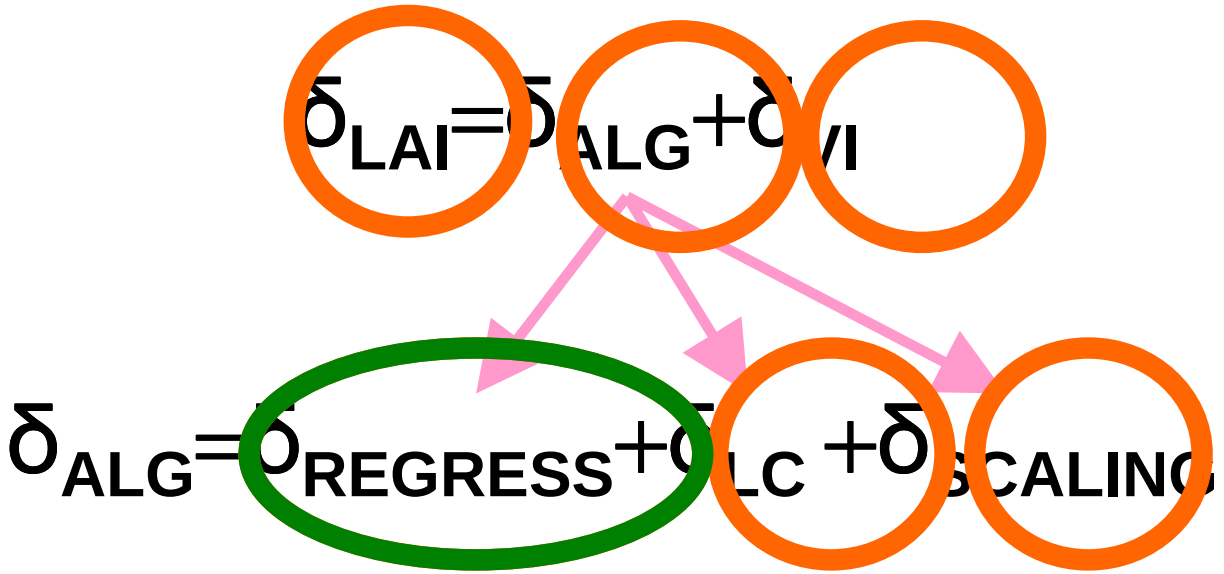

Fernandes et al., 2003, CJRS

Validation A: Errors in land cover classifications and aggregation of images (Acadia site example)

VGT LAI

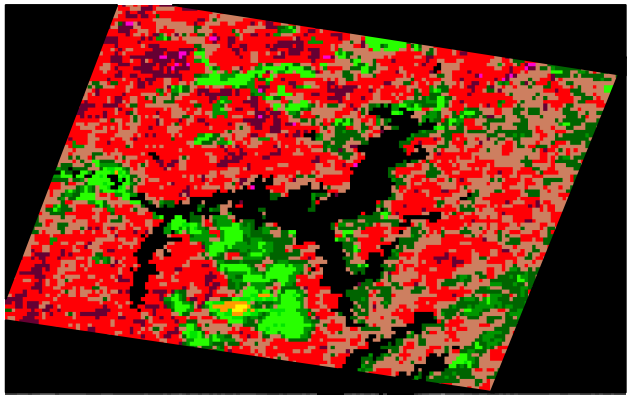

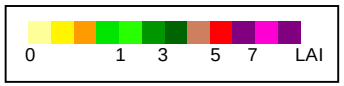

ACADIA

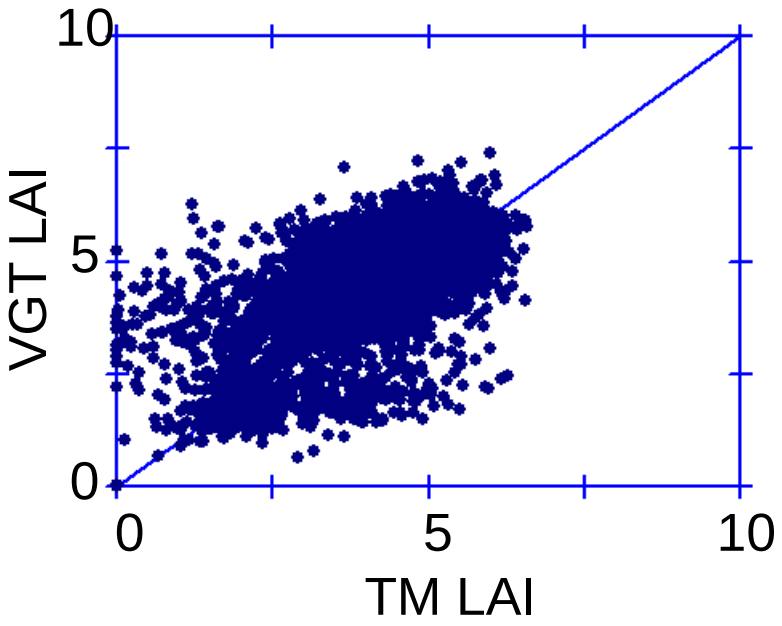

TM LAI

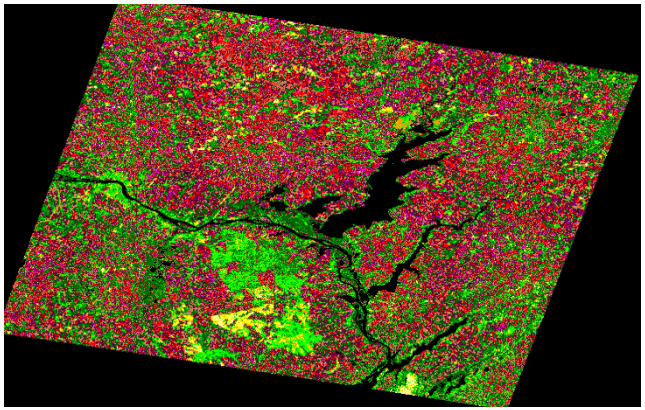

$R^2 = 0.54$, RMSE = 1.09

Pisek et al., 2007, CJRS

Validation A: Errors in land cover classifications and aggregation of images (Acadia site example)

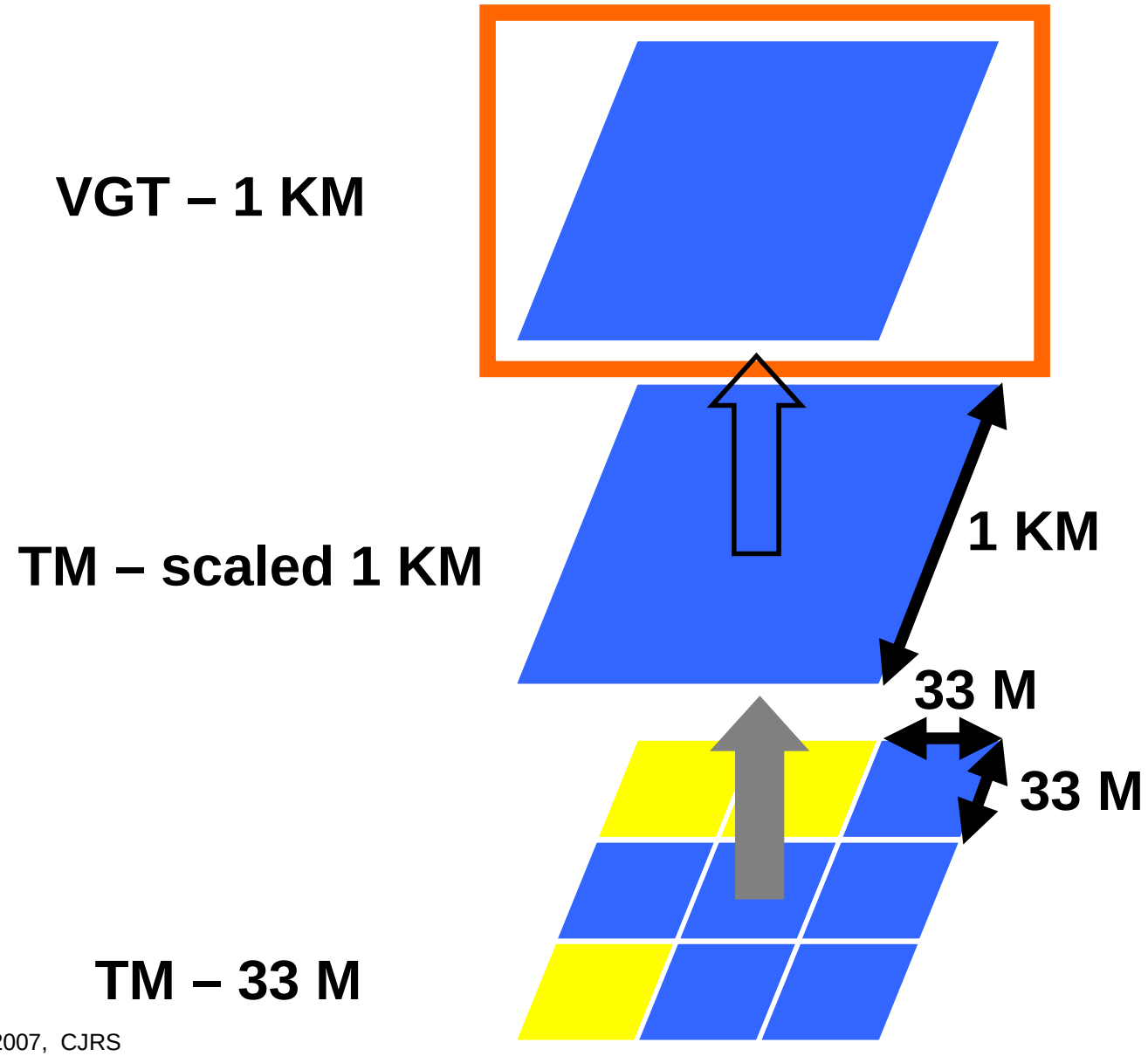

Pisek et al., 2007, CJRS

Validation A: Errors in land cover classifications and aggregation of images (Acadia site example)

DOMINANT TM LAND COVER TYPE

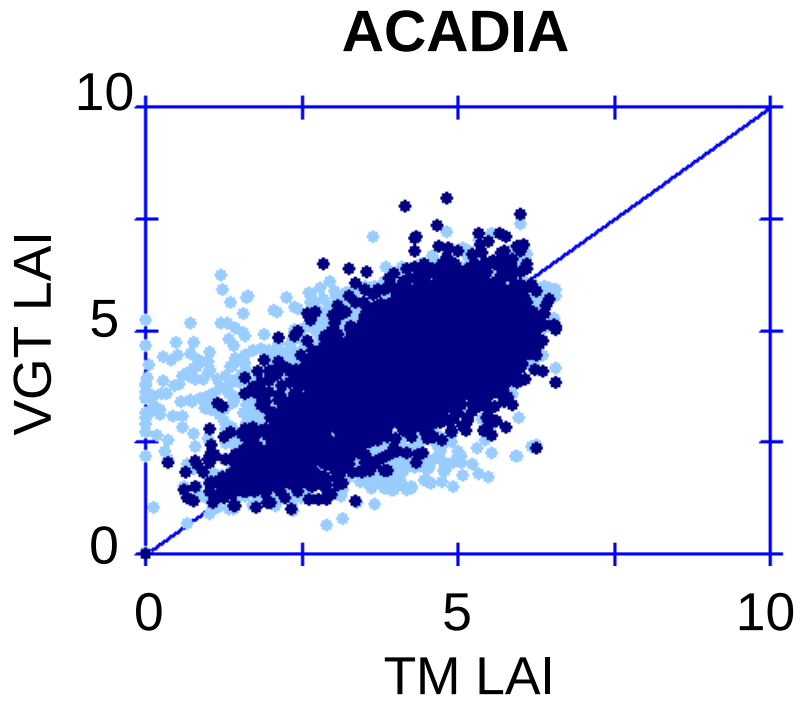

Pisek et al., 2007, CJRS

R^2 = 0.65, RMSE = 0.87

Validation A: Errors in land cover classifications and aggregation of images (Acadia site example)

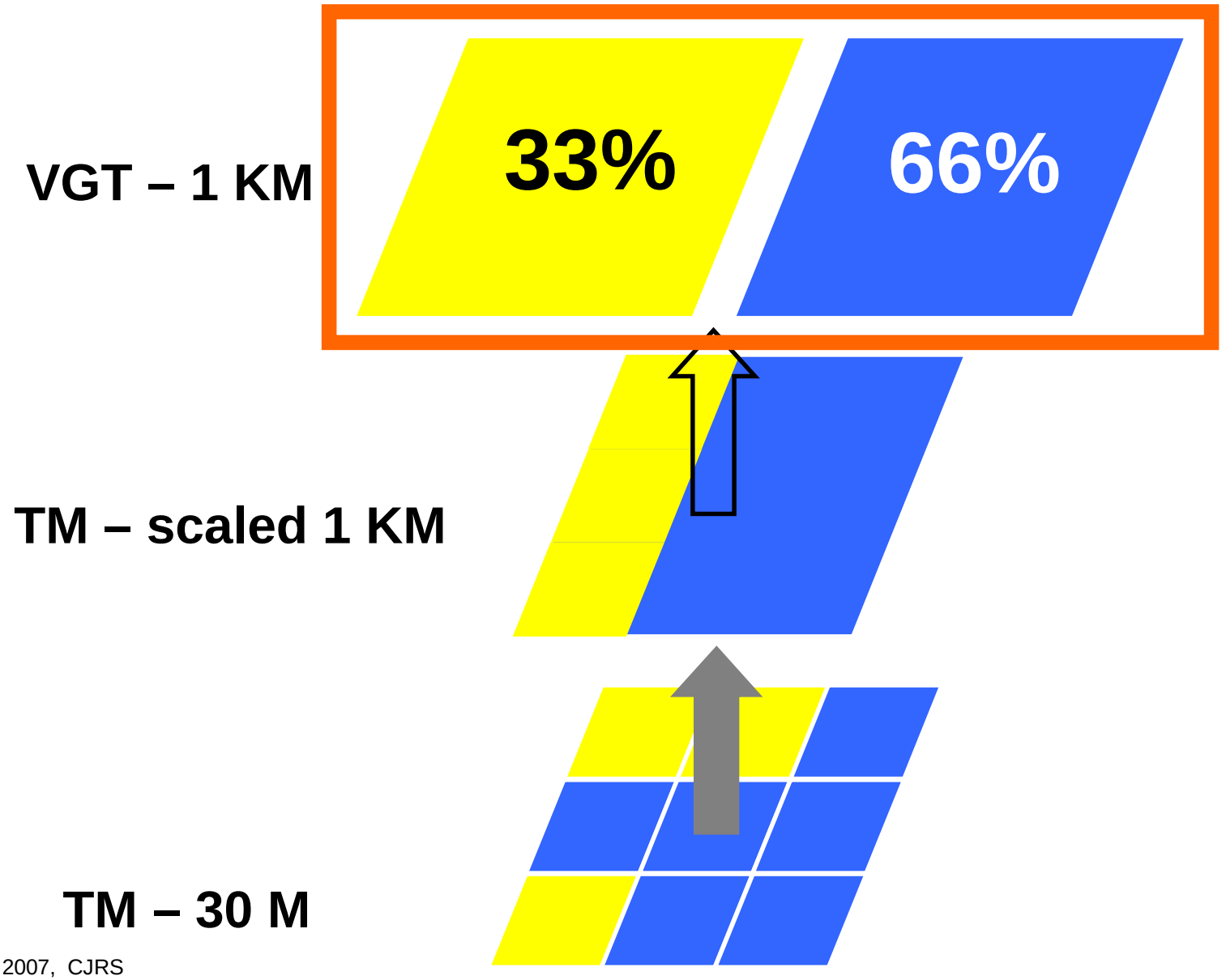

Pisek et al., 2007, CJRS

Validation A: Errors in land cover classifications and aggregation of images (Acadia site example)

WEIGHTED TM LAND COVER INFORMATION

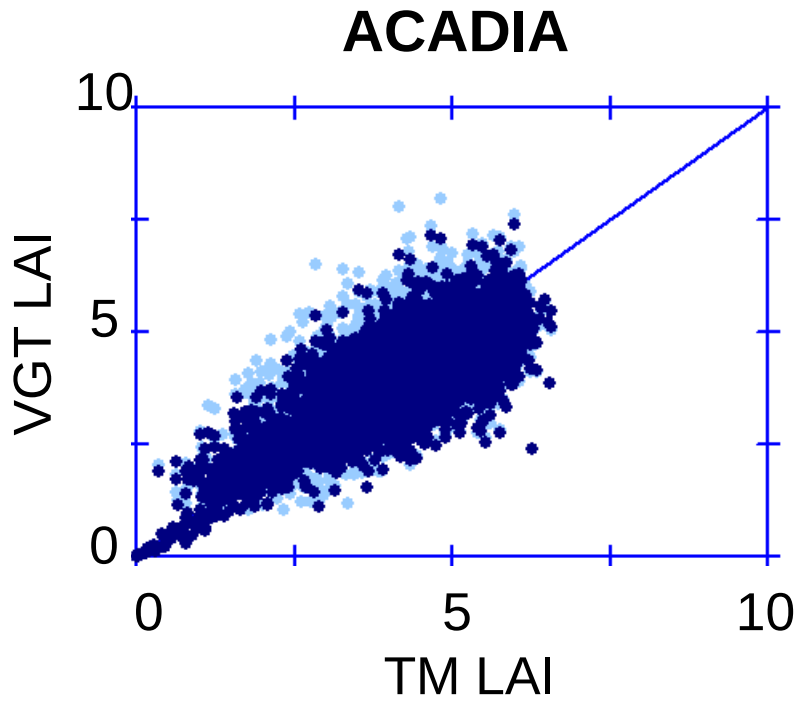

Pisek et al., 2007, CJRS

$R^2 = 0.76$, RMSE = 0.72

Validation A: Errors in land cover classifications and aggregation of images (Acadia site example)

BOTH VGT AND TM AGGREGATED TO 4 KM RES.

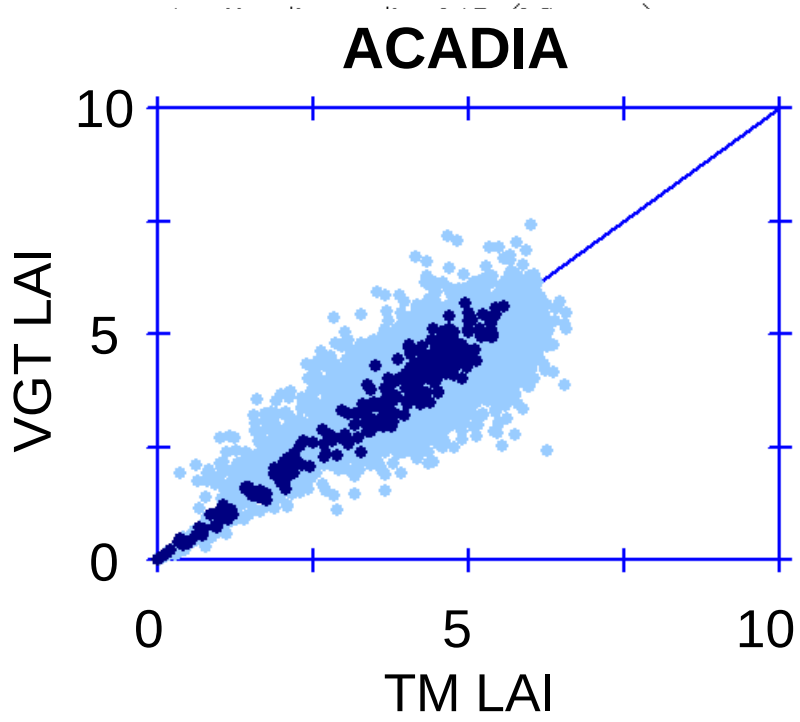

R^2 = 0.96, RMSE = 0.3

Pisek et al., 2007, CJRS

Validation B: MODIS/VGT LAI comparison

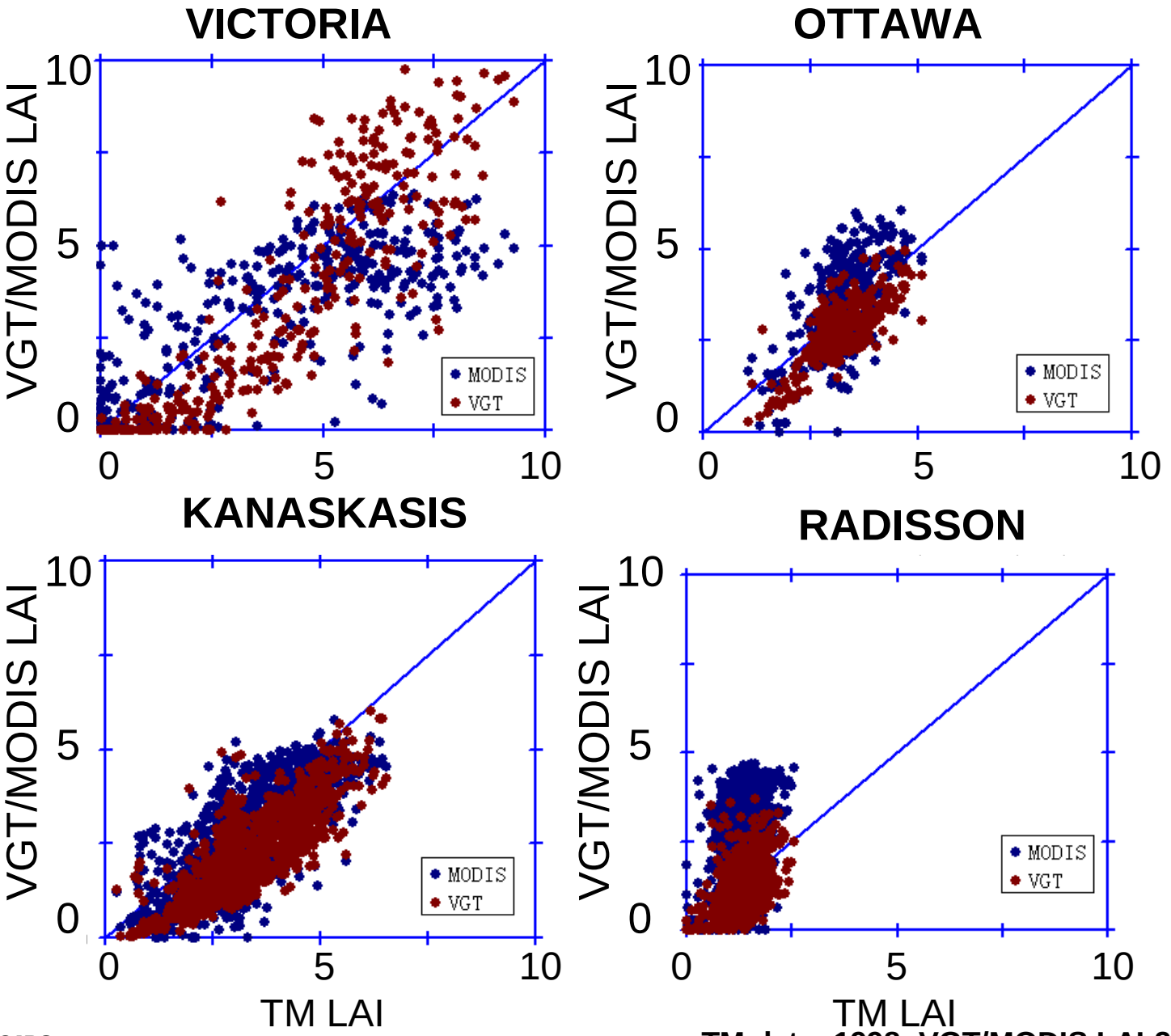

Pisek et al., 2007, CJRS

TM data: 1998; VGT/MODIS LAI:2003

Validation B: BigFoot sites

- used 4 sites :AGRO, HARV, KONZ, NOBS

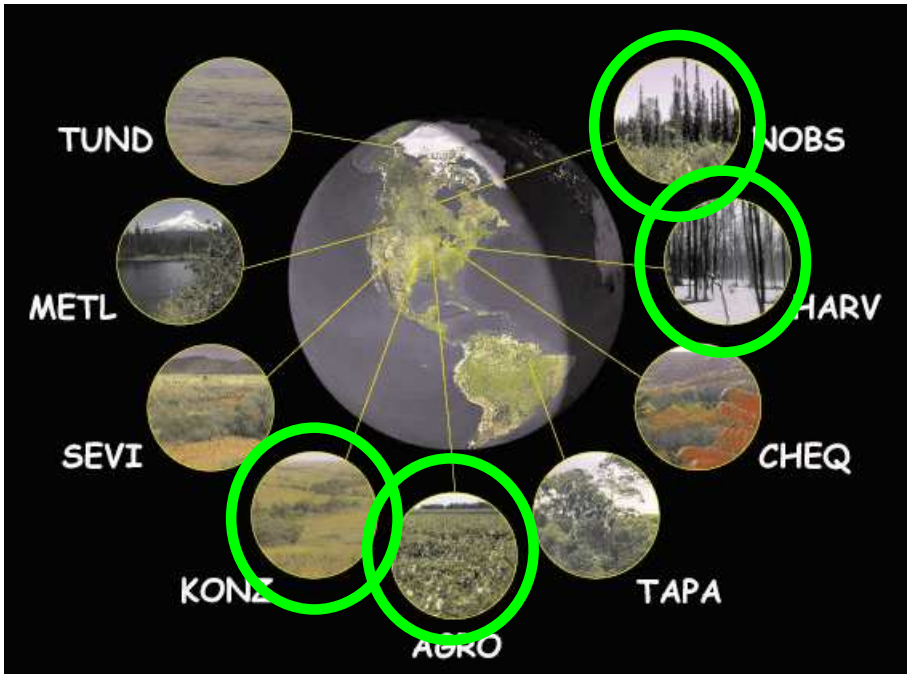

-BigFoot TM scenes: (http://www.fsl.orst.edu/larse/bigfoot/)

-MODIS ASCII subsets: (http://www.modis.ornl.gov/modis/index.cfm)

Annual LAI cycle 2000

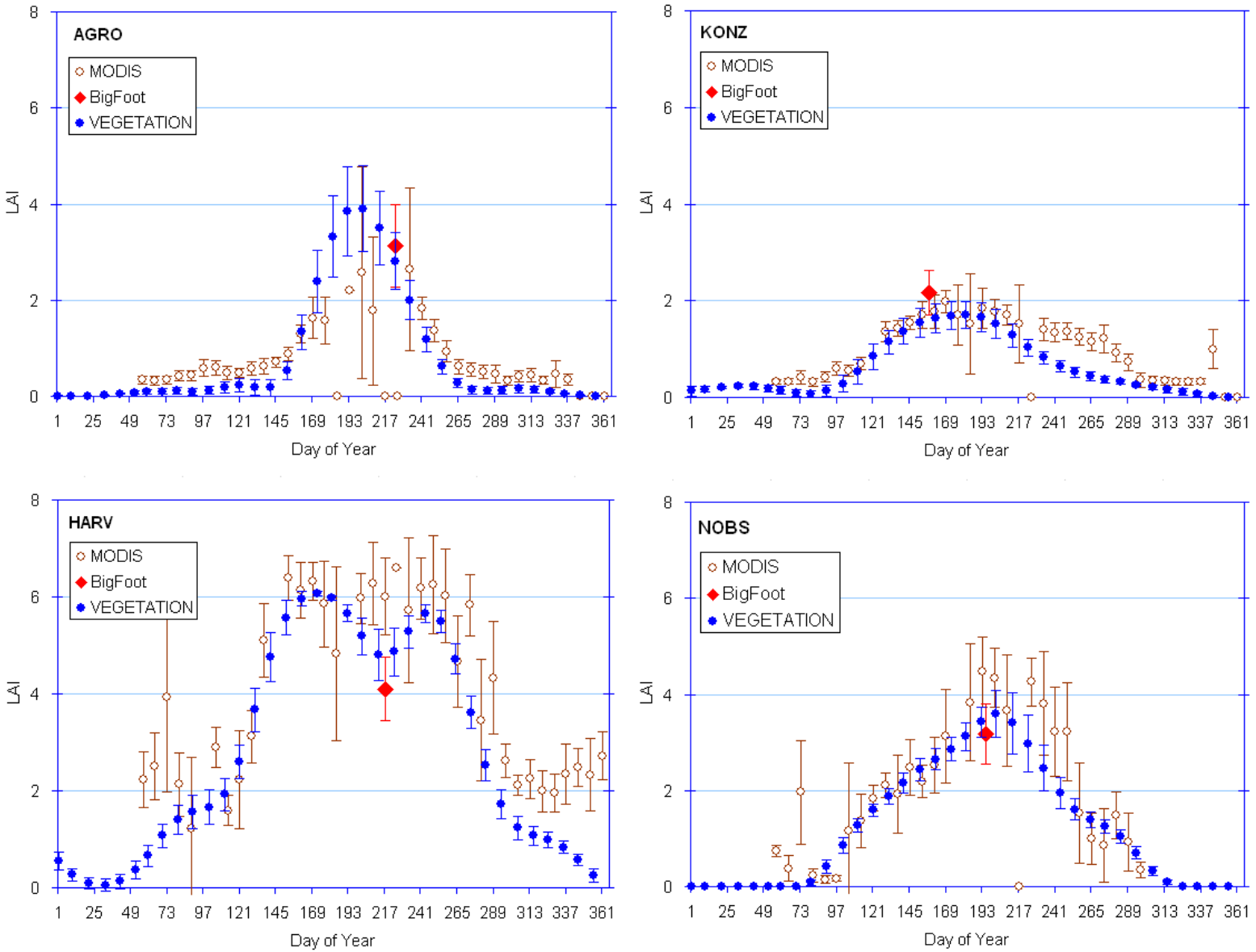

Pisek and Chen, 2007, RSE

What is leaf area index (LAI)?

- one half of the total all-sided green leaf area per unit horizontal ground surface area (Chen and Black, 1992)

LAI = 2.25

LAI = 4.75

- Key variable in ecosystem productivity models, global models of climate, fluxes of energy and mass

- The most comprehensive intercomparison study of global LAI products up to this date - Garrigues et al. (2008, JGR):
- '…..Beside the quality of surface reflectances, the global LAI products need to be improved by better accounting for the vegetation structure, namely the effects of the background and foliage clumping.'

Making the case for the multi-angle data:

The angular variations of radiometric signal: **Noise** or **Information** **?**

- **Multi-angle sampling provides sensitivity to vegetation canopy structure through the physical phenomena of shadow-hiding and volume scattering by leaves**
- **Multi-angle data are best interpreted through canopy reflectance models, which have greater explanatory power than empirical measures**
- **However, interpretation is difficult because the real world is complex and complex models can be difficult, impractical, or even impossible to invert: We have to decide on the appropriate level of complexity, or devise appropriate inversion protocols (e.g., injection of *a priori* knowledge)**

What is forest background and why do we bother?

- understory vegetation, senescent leaves, and moss/soil

- neglecting the understory has an impact on the relationship between LAI and reflectance data

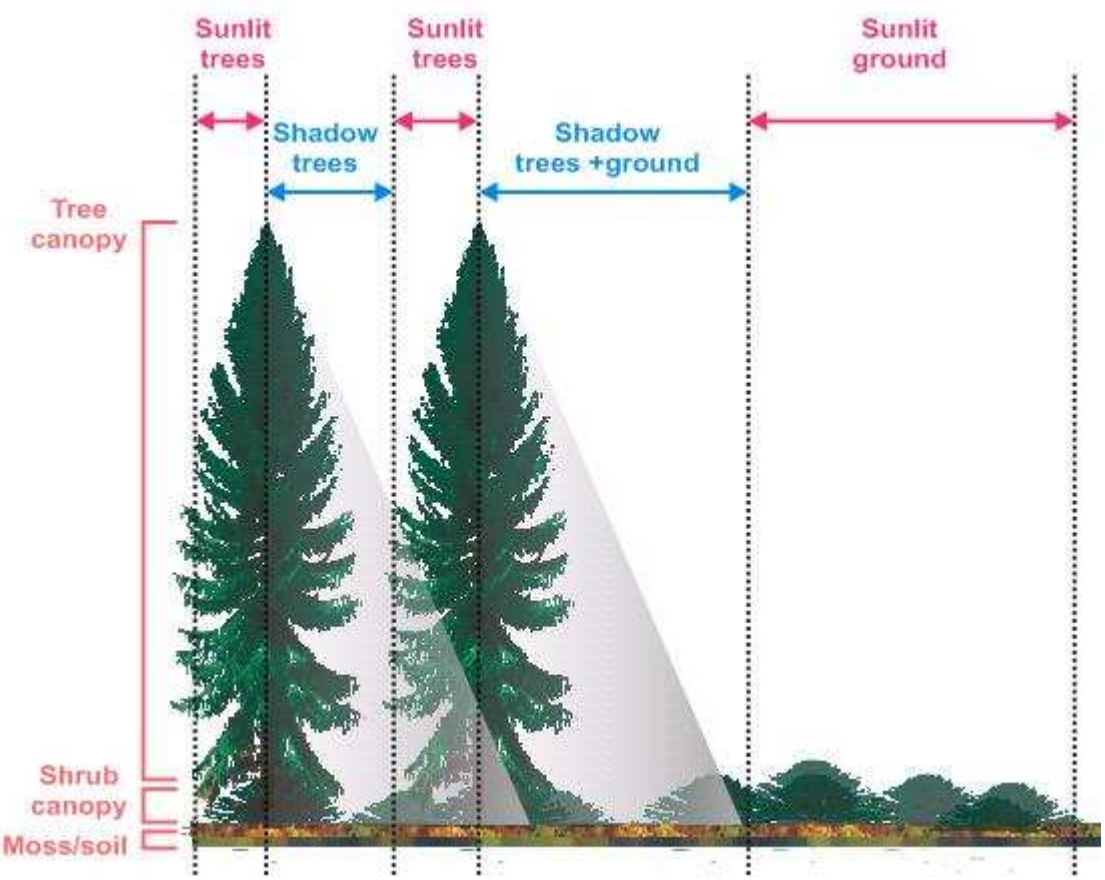

scheme after Sonnentag et al., 2007, RSE

Calculating background reflectance

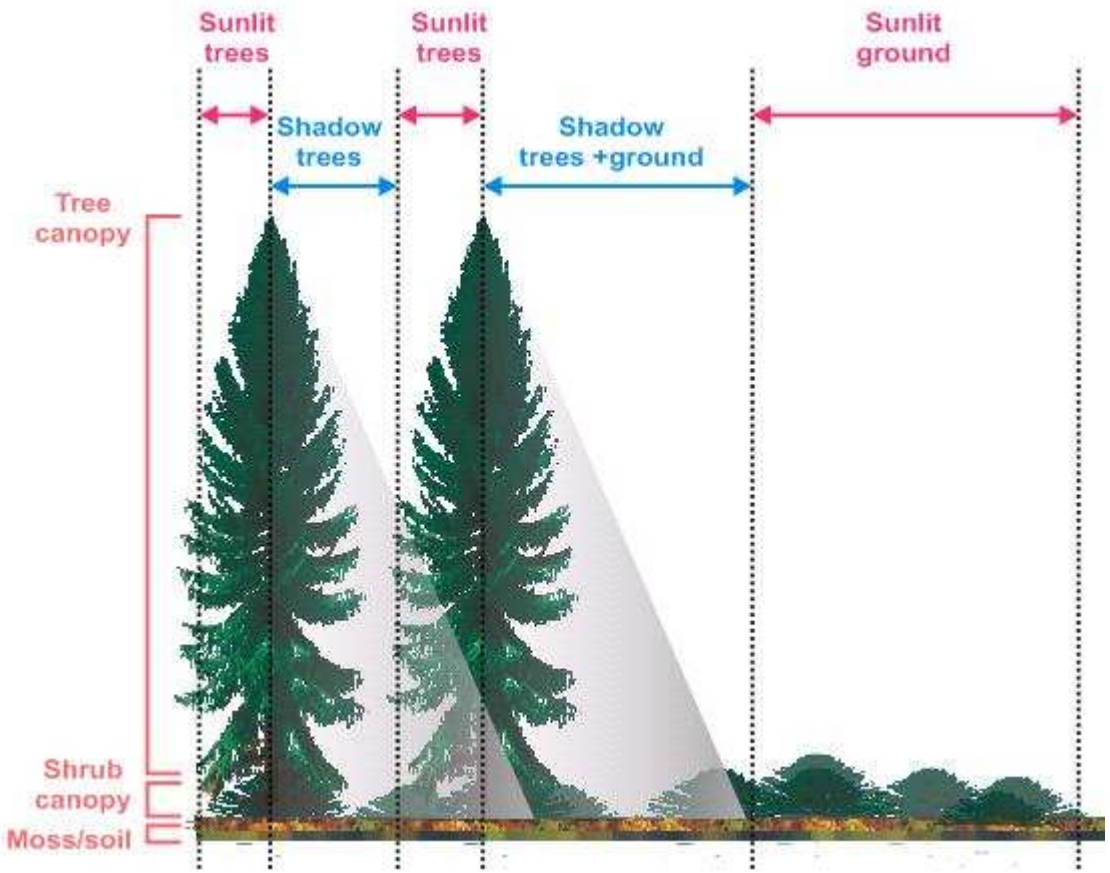

$$R_b = P_{tb} \times R_T + P_{gb} \times R_G + Z_{tb} \times R_{ZT} + Z_{gb} \times R_{ZG}$$

Calculating background reflectance

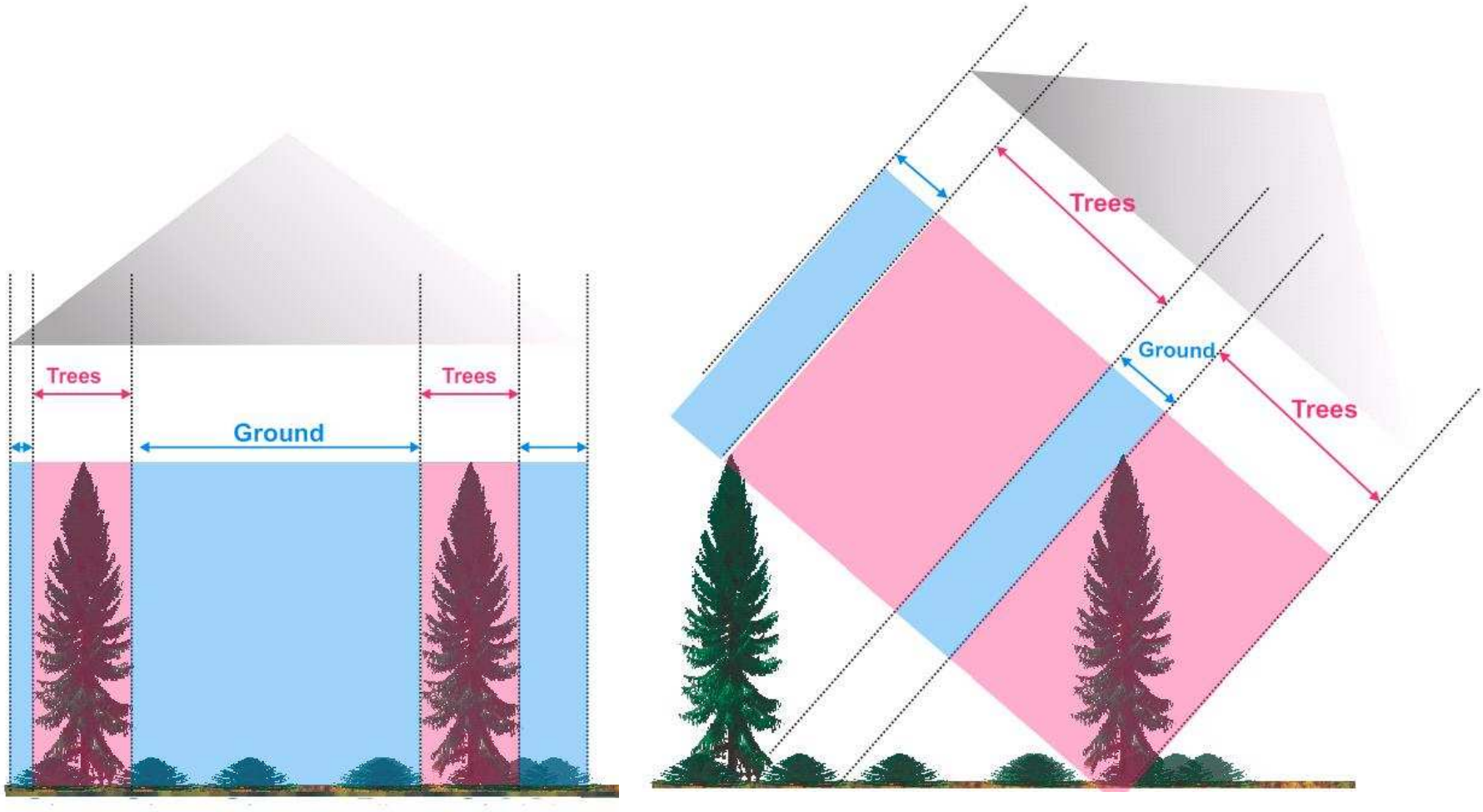

$$R_d = P_{to} \times R_T + P_{go} \times R_G + Z_{to} \times R_{ZT} + Z_{go} \times R_{ZG}$$

$$R_d = P_{ts} \times R_T + P_{gs} \times R_G + Z_{ts} \times R_{ZT} + Z_{gs} \times R_{ZG}$$

$$R_{ZT} = M R_T ; R_{ZG} = M R_G$$

Canisius and Chen, 2007; Pisek et al., 2010, IEEE-TGRS

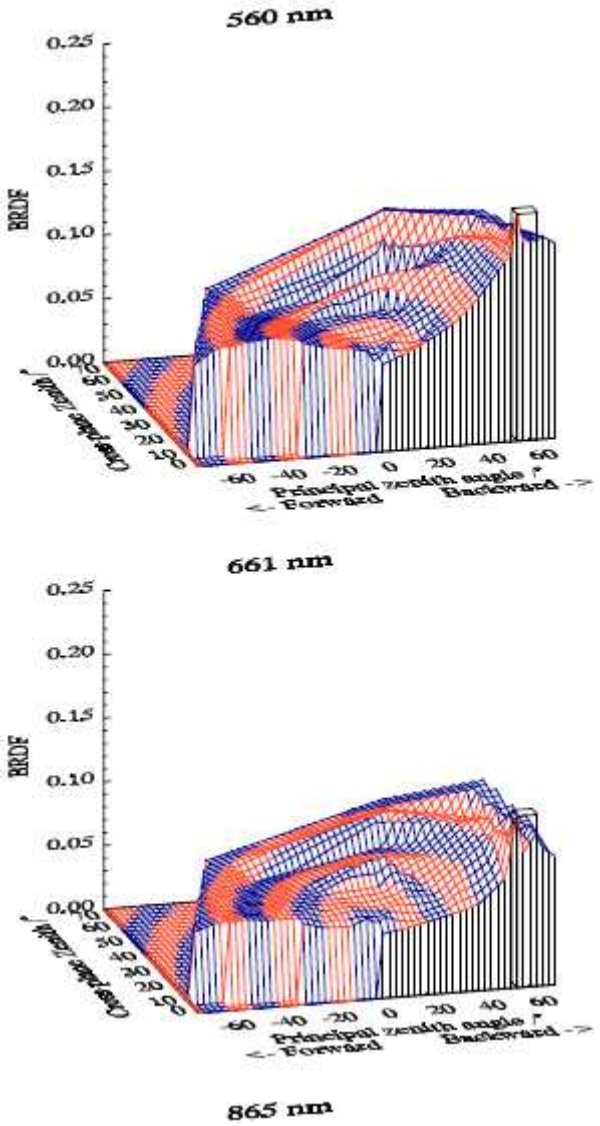

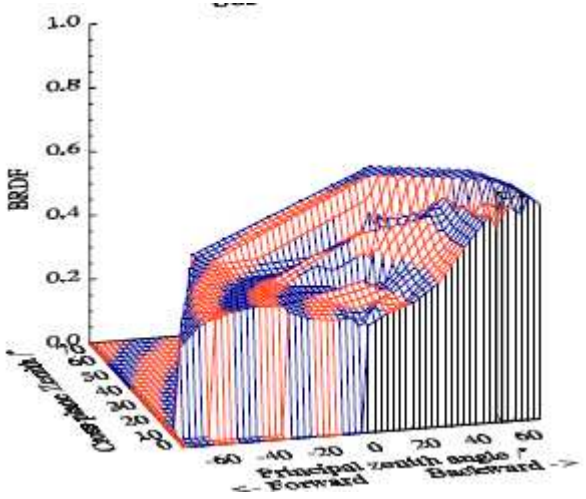

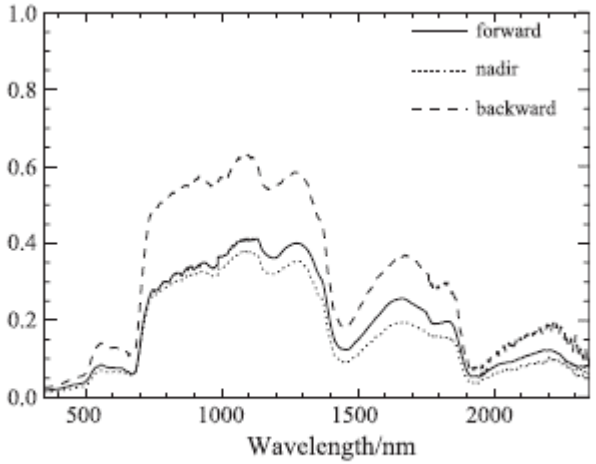

Fig. 19. The spectra of mixed understory (0°, ±50°). Lamp zenith angle is 58°.

Peltoniemi et al., 2005, RSE

Measuring/modifying understory in northern Ontario in June 2007; CASI setup

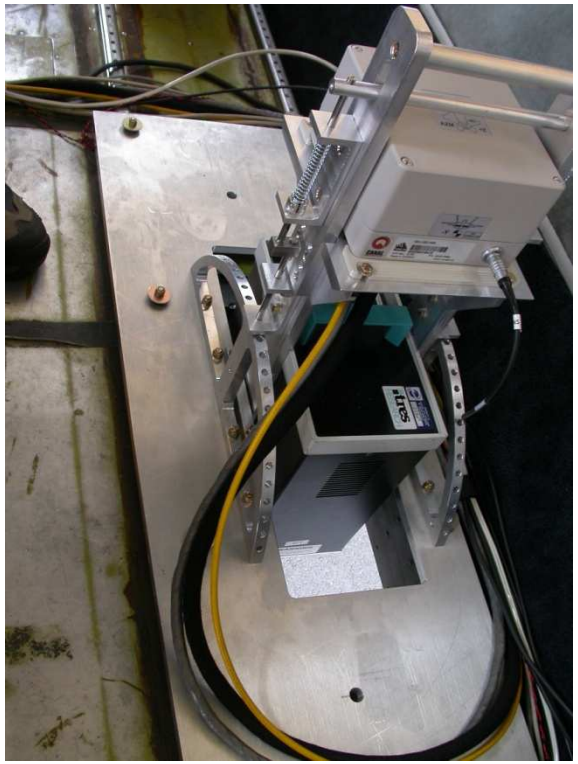

CASI – push-broom scanner

- operated in hyperspectral mode (7.5 nm bandwidth)
- 2 m spatial resolution; scene observed at **nadir** and at **40 degrees forward**
- Data scaled up to 20 m resolution, bands aggregated to simulate MISR-like red and NIR bands

Pisek et al., 2010, IEEE

Background influence on total reflectance

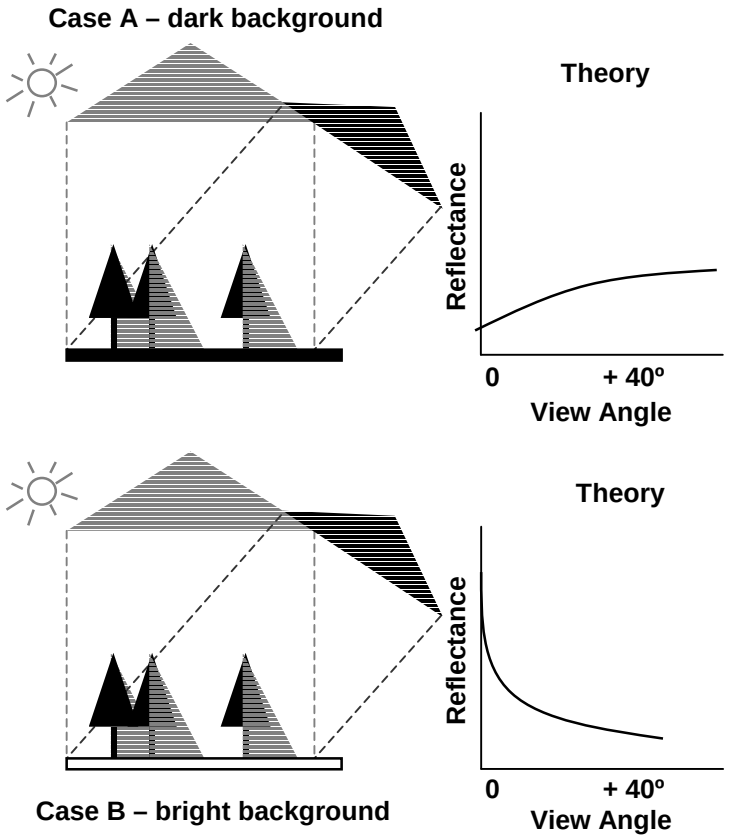

Pisek et al., 2010, IEEE

Background influence on total reflectance

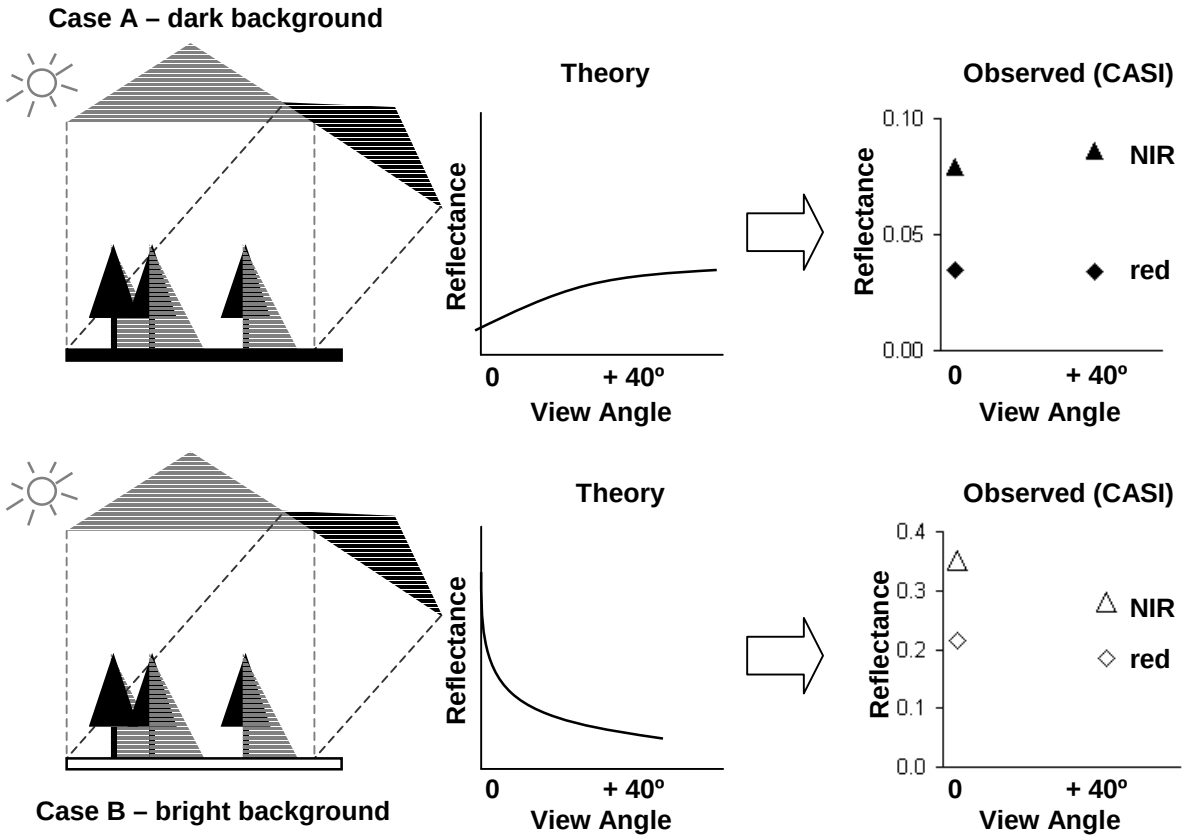

Pisek et al., 2010, IEEE

CASI background reflectances vs. ground observations

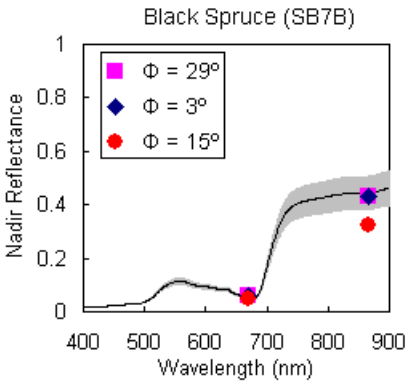

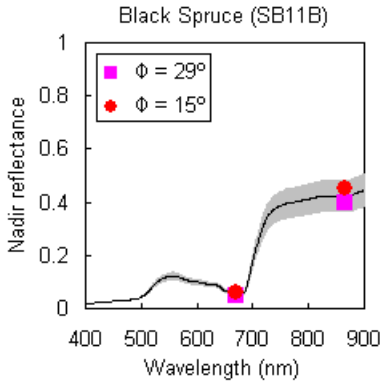

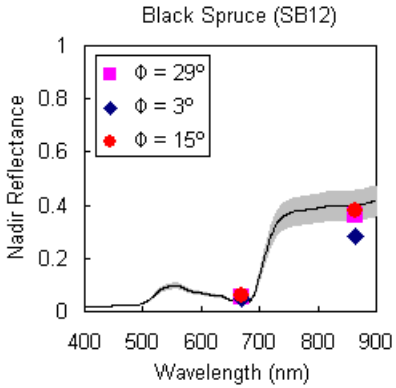

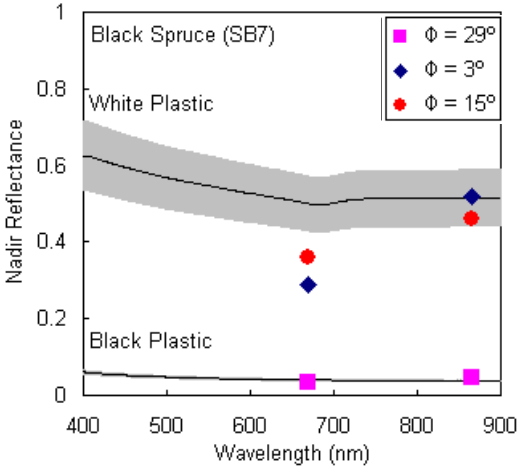

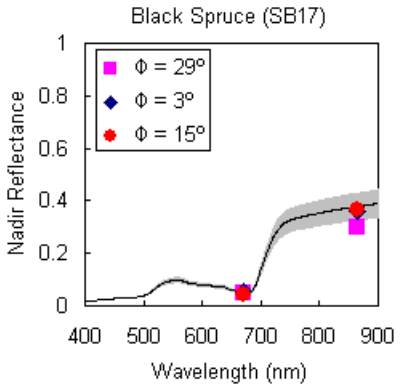

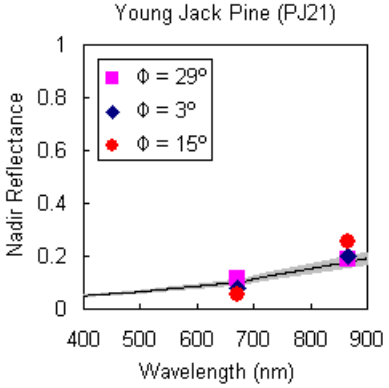

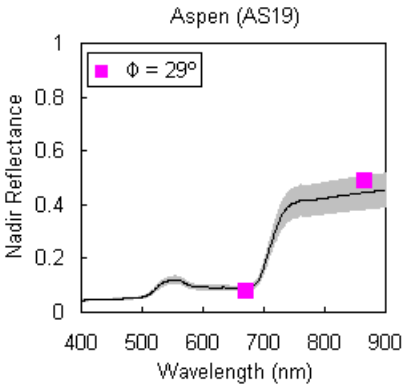

Pisek et al., 2010, IEEE

White plastic problem

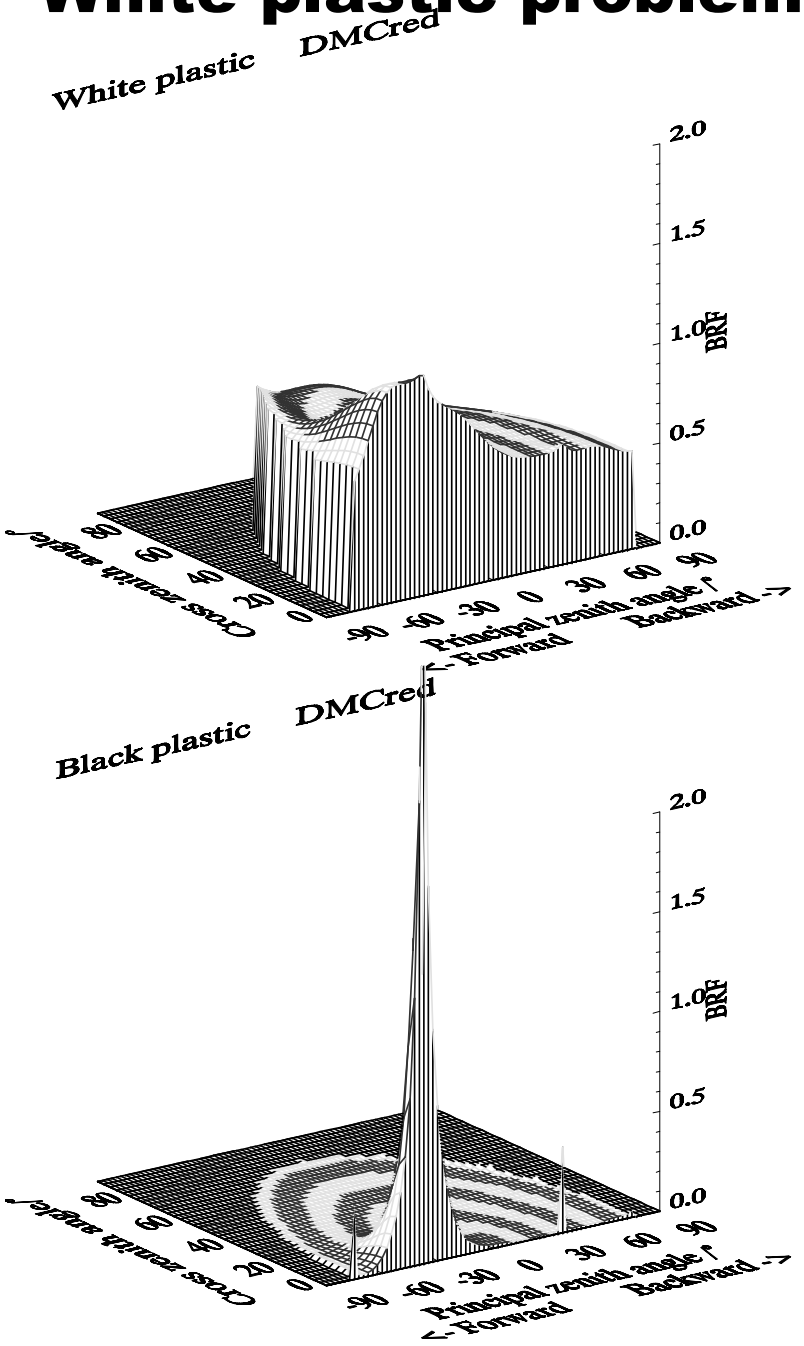

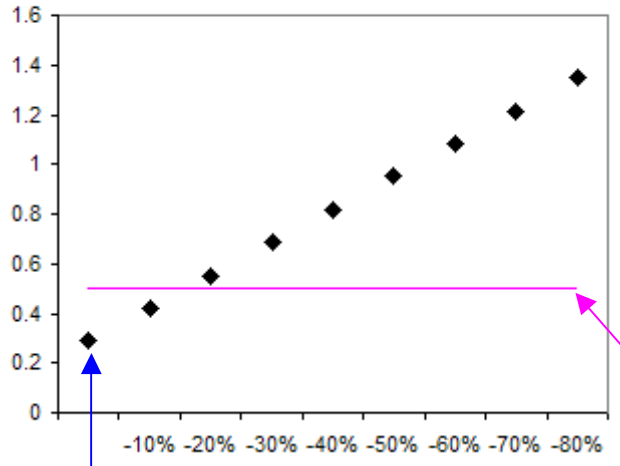

Measured Angular Reflectance by CASI

Measured Reflectance by ASD

Pisek et al., 2010, IEEE

NASA Multiangle Imaging SpectroRadiometer (MISR)

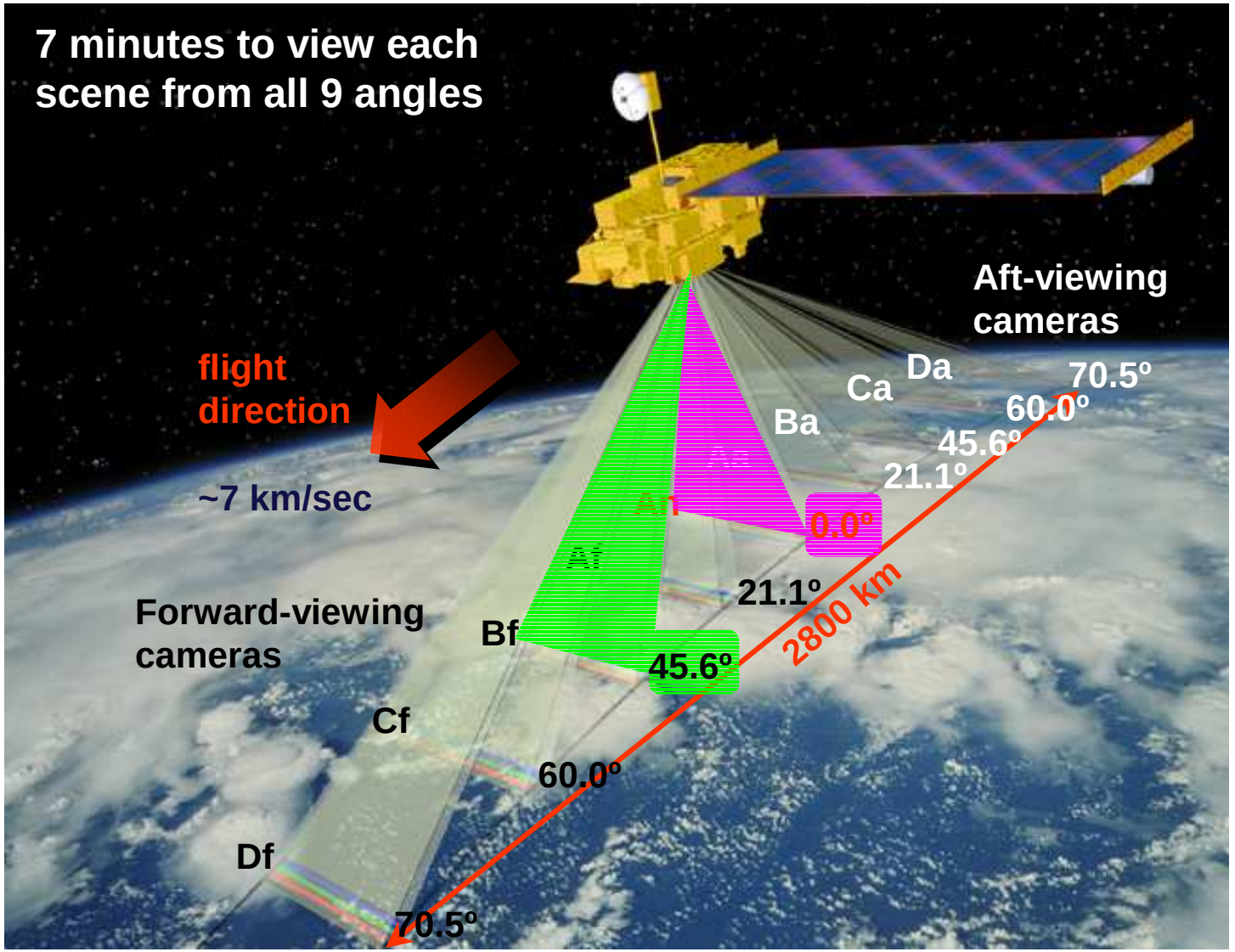

- calibrated measurements of the intensity of reflected light in 9 views and 4 wavelengths

(scheme modified from David J. Diner, JPL, Caltech, Workshop, May 22, 2005 and Chopping, 2006; 3rd Global Vegetation Workshop, Missoula, MT)

Forest Background Reflectance–Red Band MISR 2007 (AN and BF cameras)

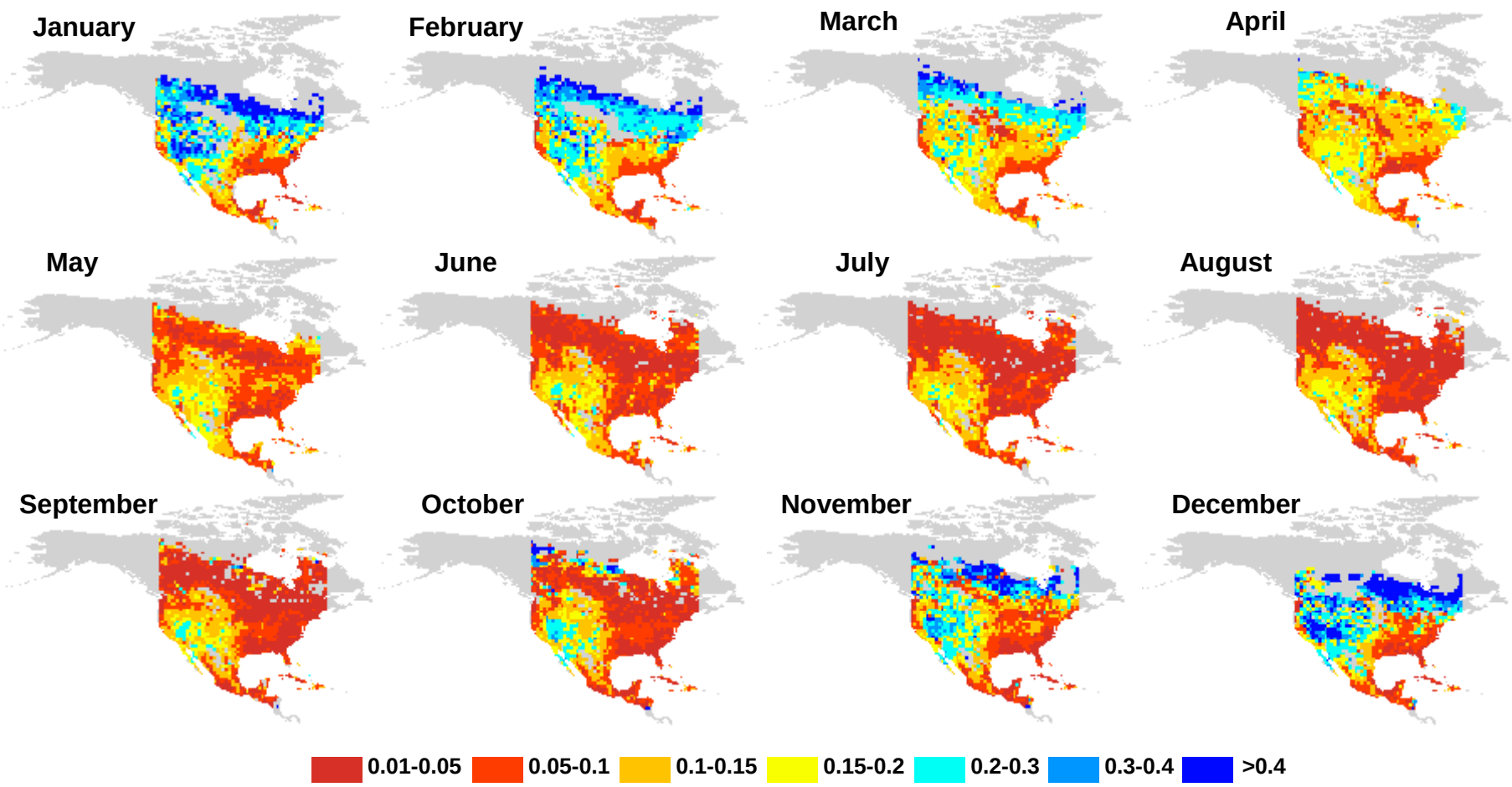

Pisek and Chen, 2009, RSE

What is clumping index (Ω)?

- quantifies the degree of the deviation of foliage spatial distribution from the random case

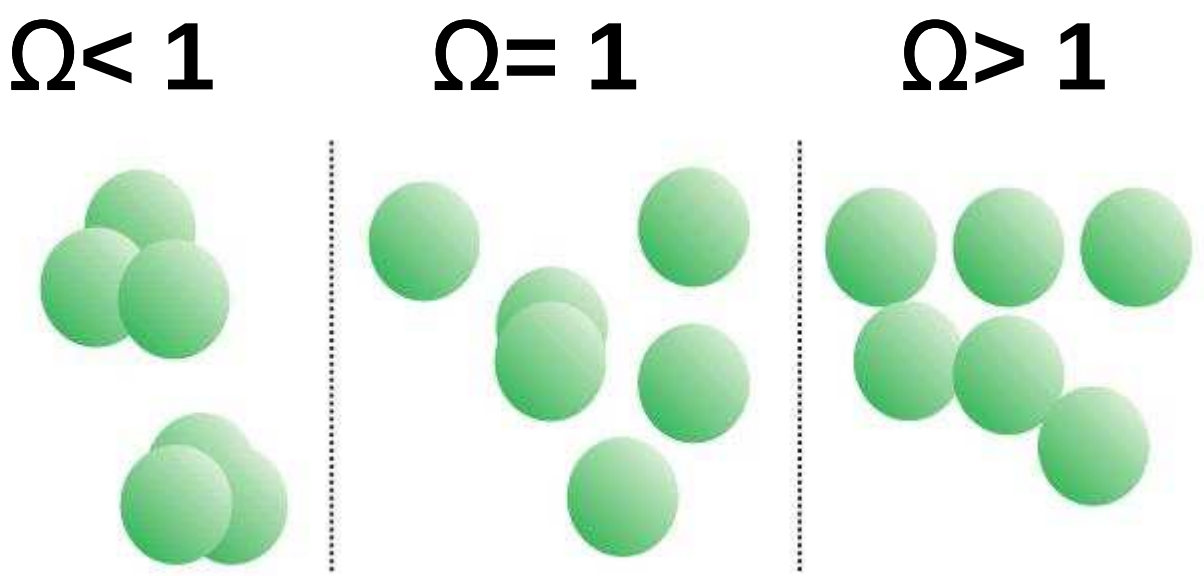

Bidirectional Reflectance Distribution Function (BRDF)

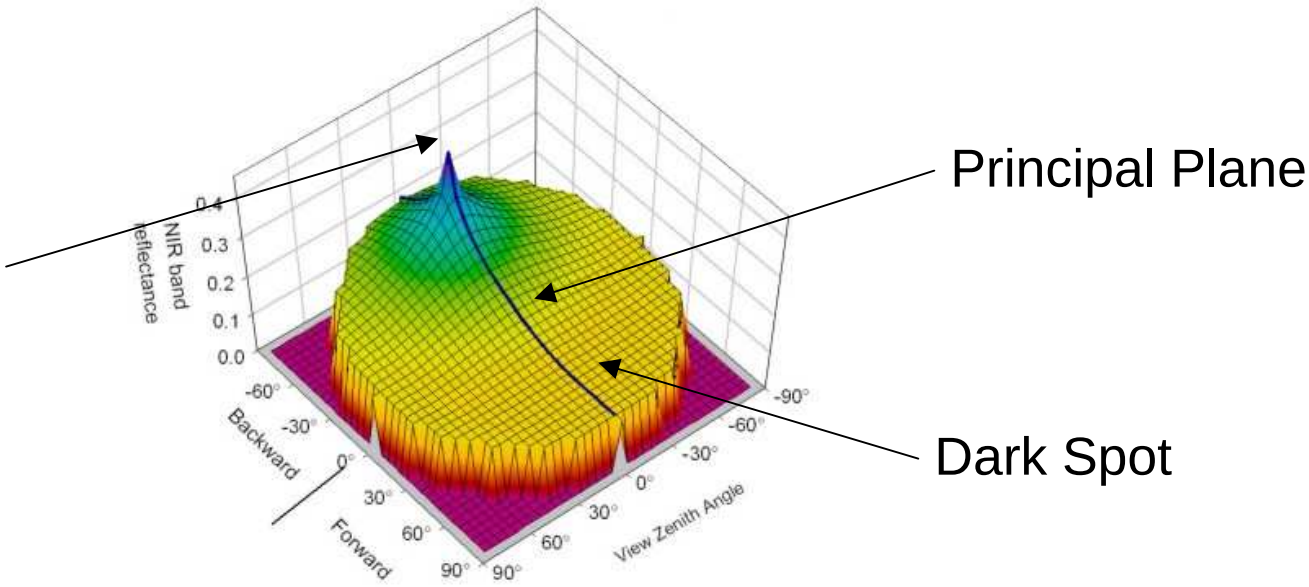

The anisotropy index (NDHD) = (HS – DS)/(HS + DS)

Chen et al., 2003, RSE

Bidirectional Reflectance Distribution function (BRDF)

POLDER Observations along the Principal Plane for 3 samples

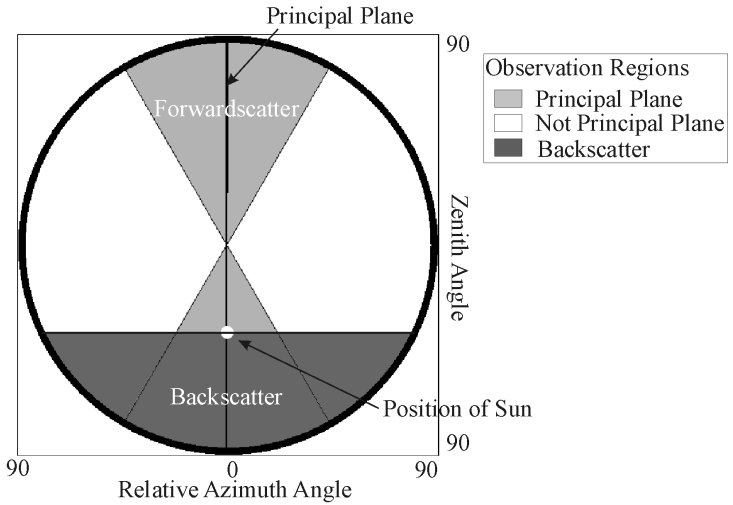

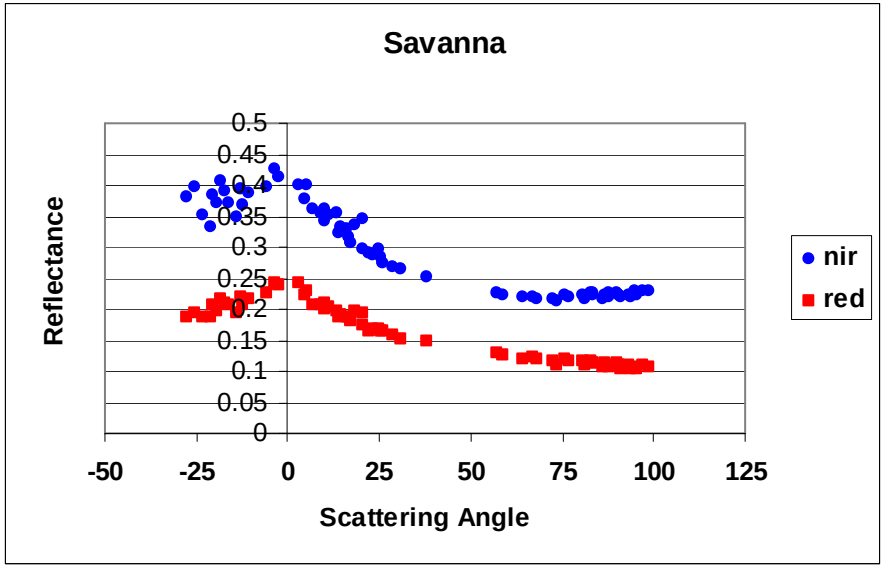

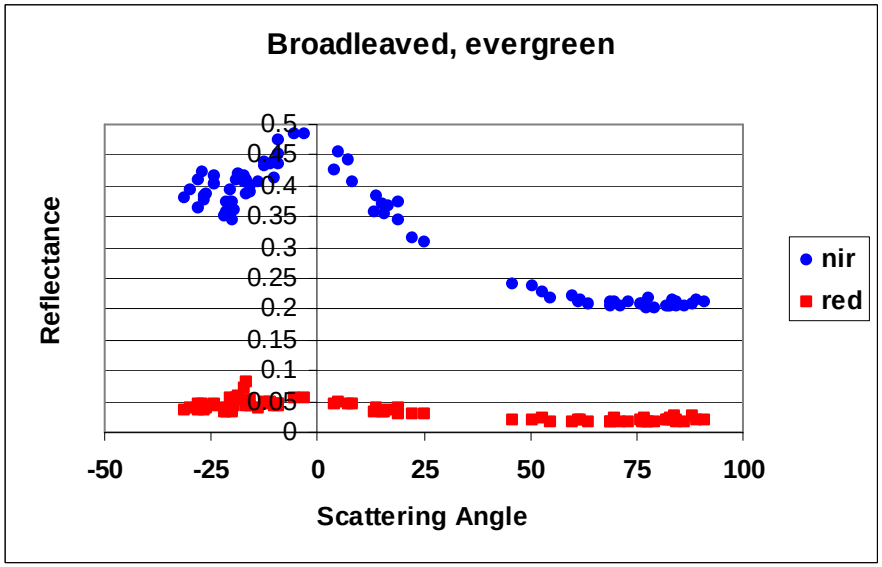

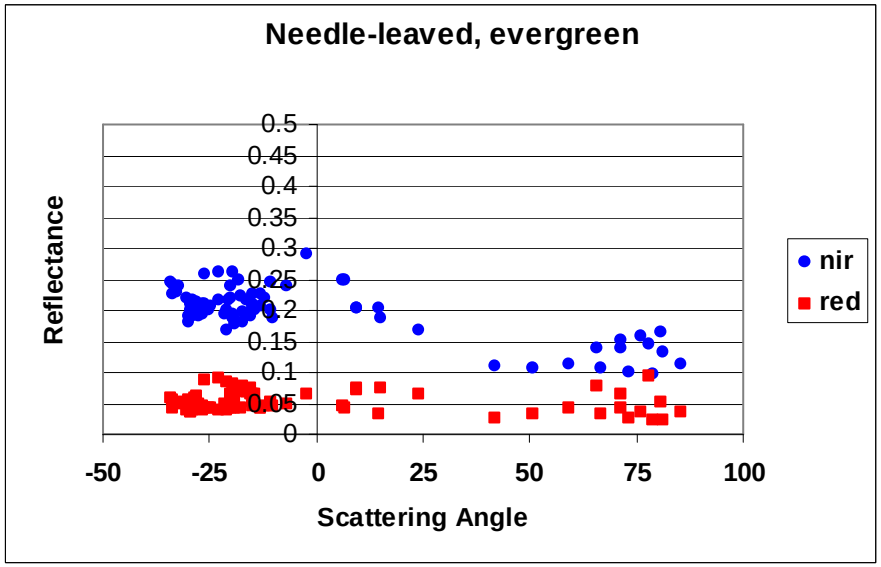

Four-Scale Model Simulation Results - NDHD vs. clumping index

Overall correlation for 10000 simulations
with canopy cover above 25%

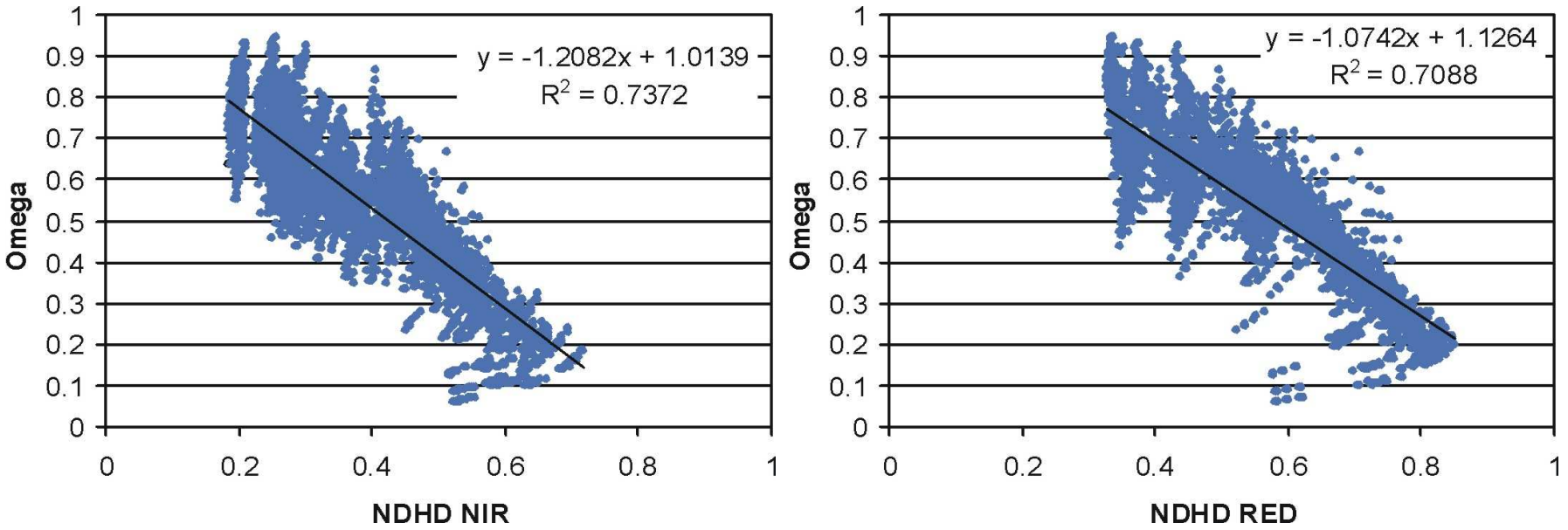

Chen et al., 2005, RSE

POLDER-1 Clumping index map
(composite period 96/11-97/06)

(Chen et al, 2005, RSE)

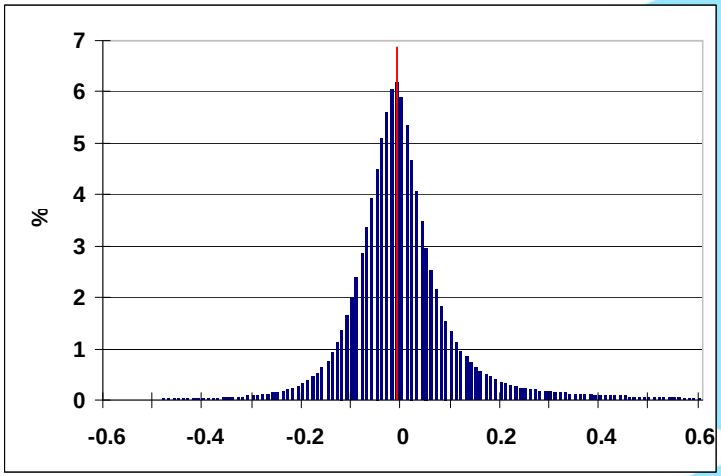

POLDER-3 Clumping index map
(composite period 05/01-05/12)

POLDER-3 Global Clumping index map

(missing areas filled with POLDER-1 estimates or averages for given land cover type)

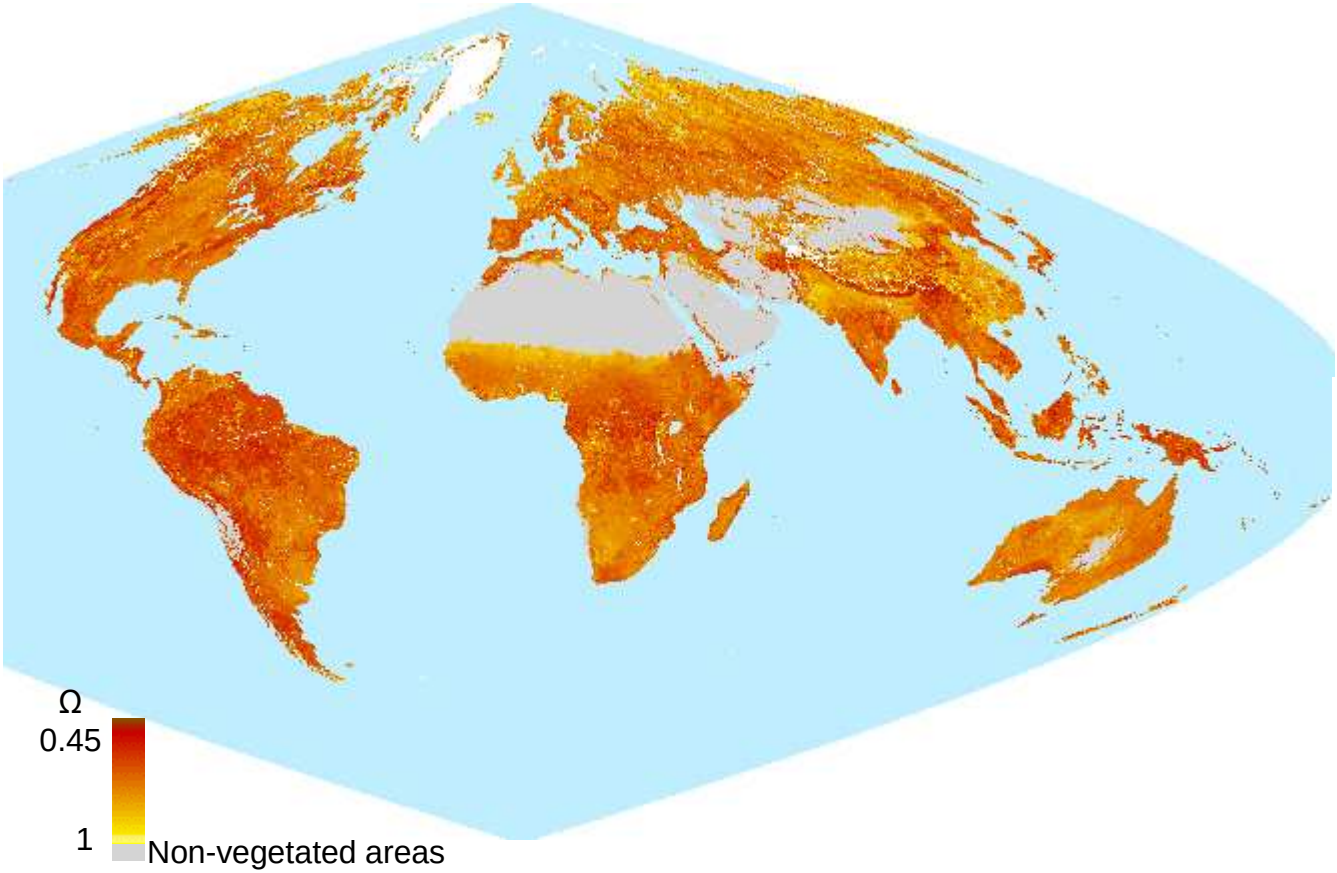

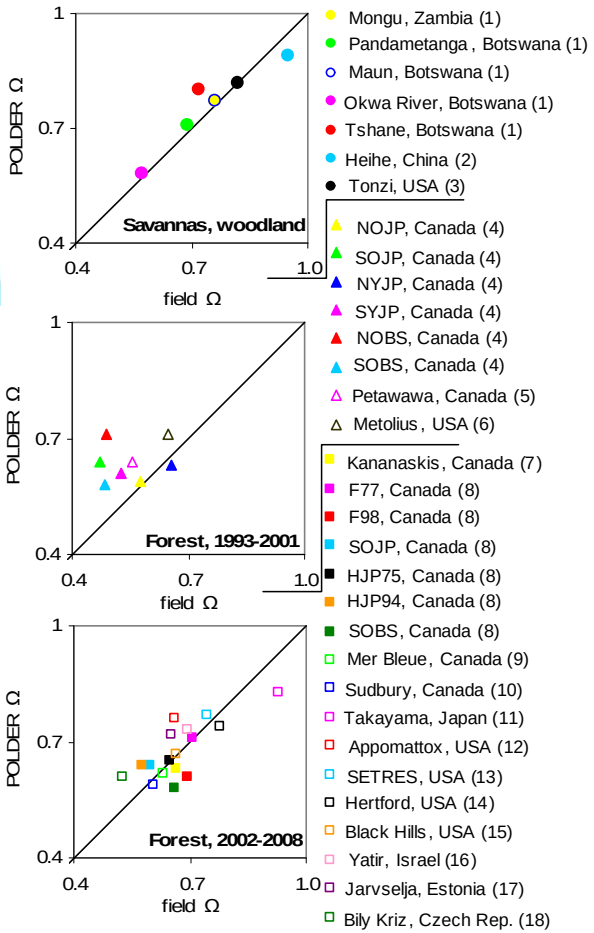

Pisek et al., 2010, ISPRS J. Photogr. Remote Sens.

VeMP (VEgetation, Misr, Polder)

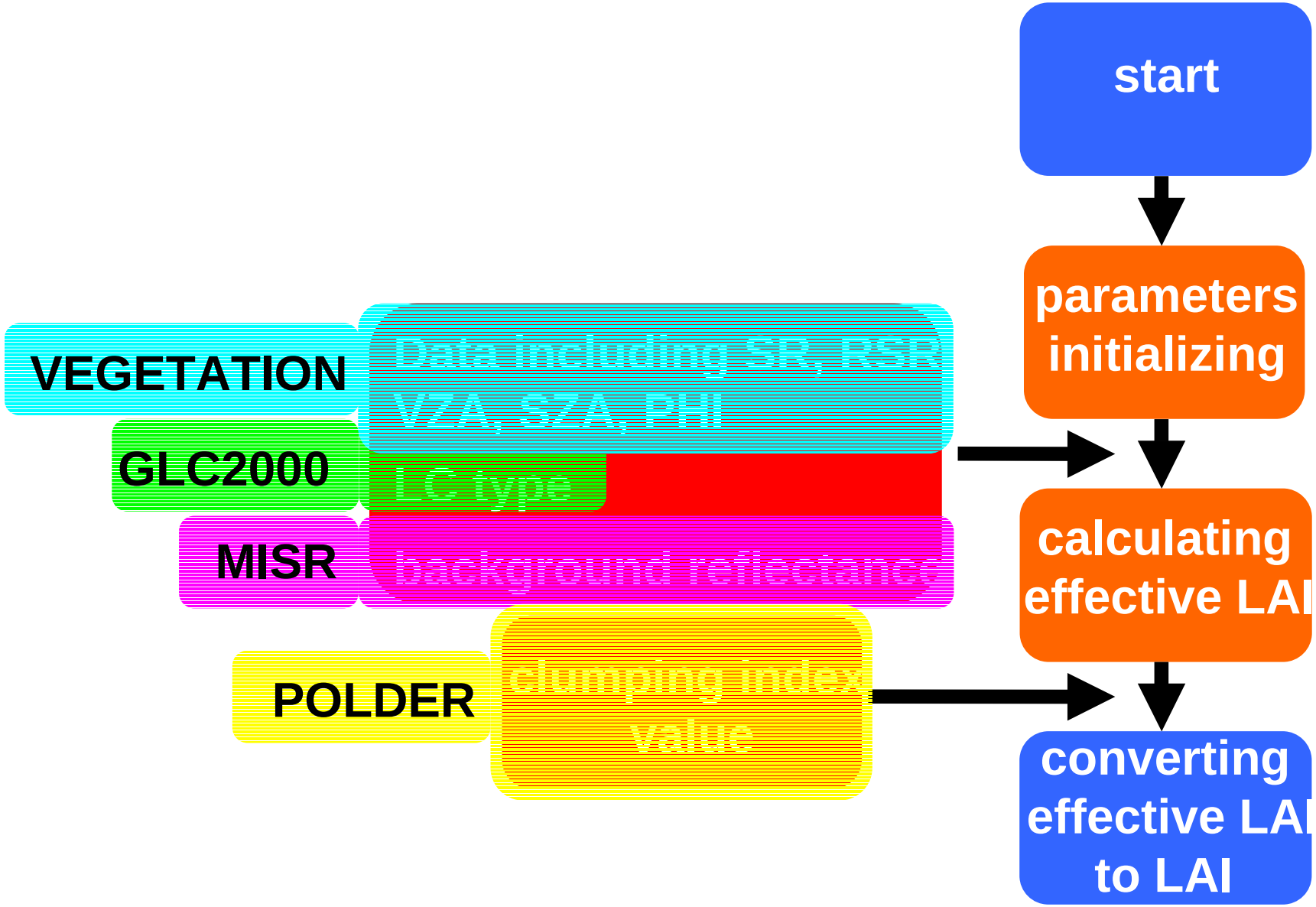

Deng et al., 2006, IEEE-TGRS; Pisek et al., 2010, JGR

Temporal consistency of LAI products

ECOCLIMAP LAI **MODIS C4 LAI** **Cyclopes LAI** (Weiss et al., 2008, RSE)

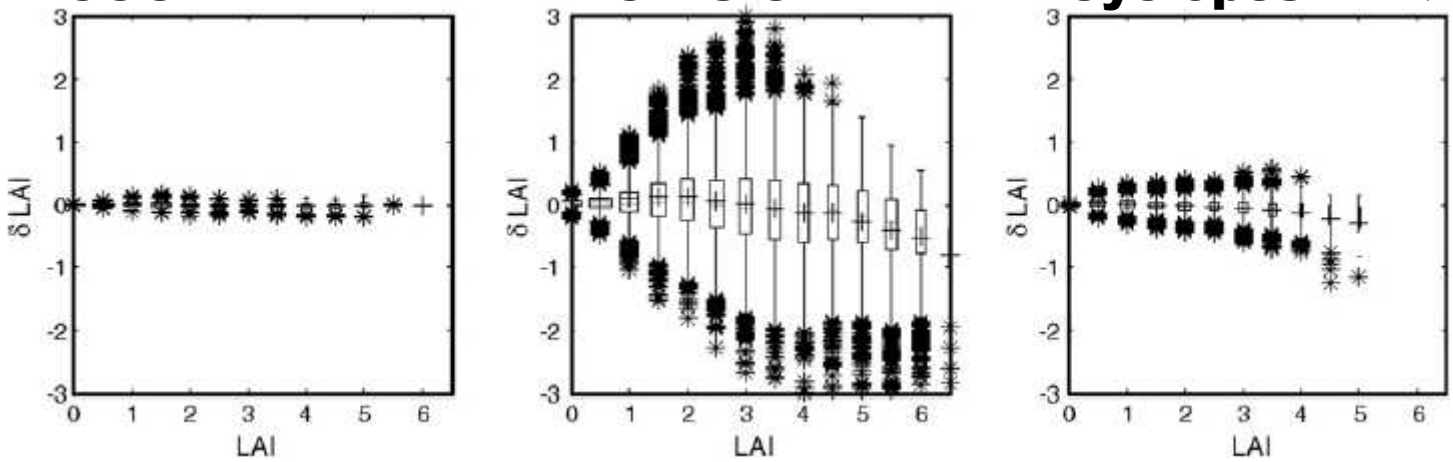

$$\delta = (1/2(LAI(t+\Delta t) + (LAI(t-\Delta t)) - LAI(t)$$

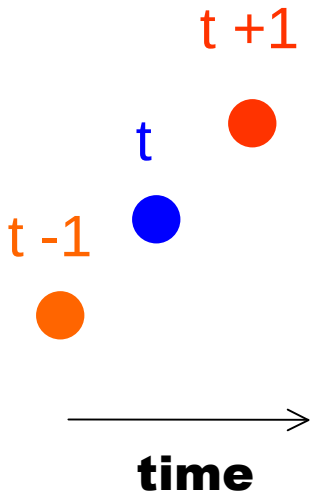

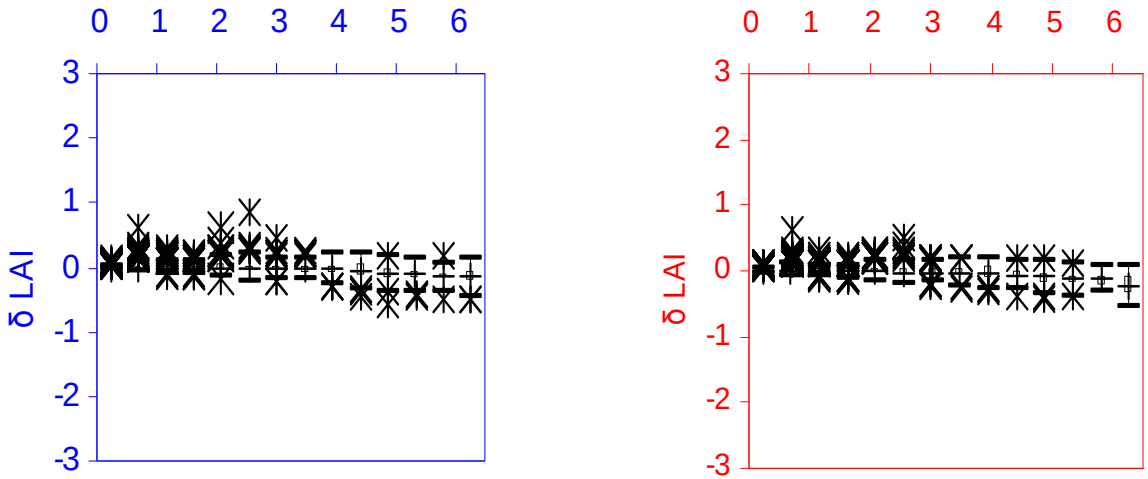

VGT LAI **VeMP LAI**

Pisek et al., 2010, JGR

LAI - June 2002

soil background
+ mean Ω for biomes
from POLDER 1

background
reflectance
from MISR
+ Ω from POLDER 1/POLDER 3

forest understory
LAI

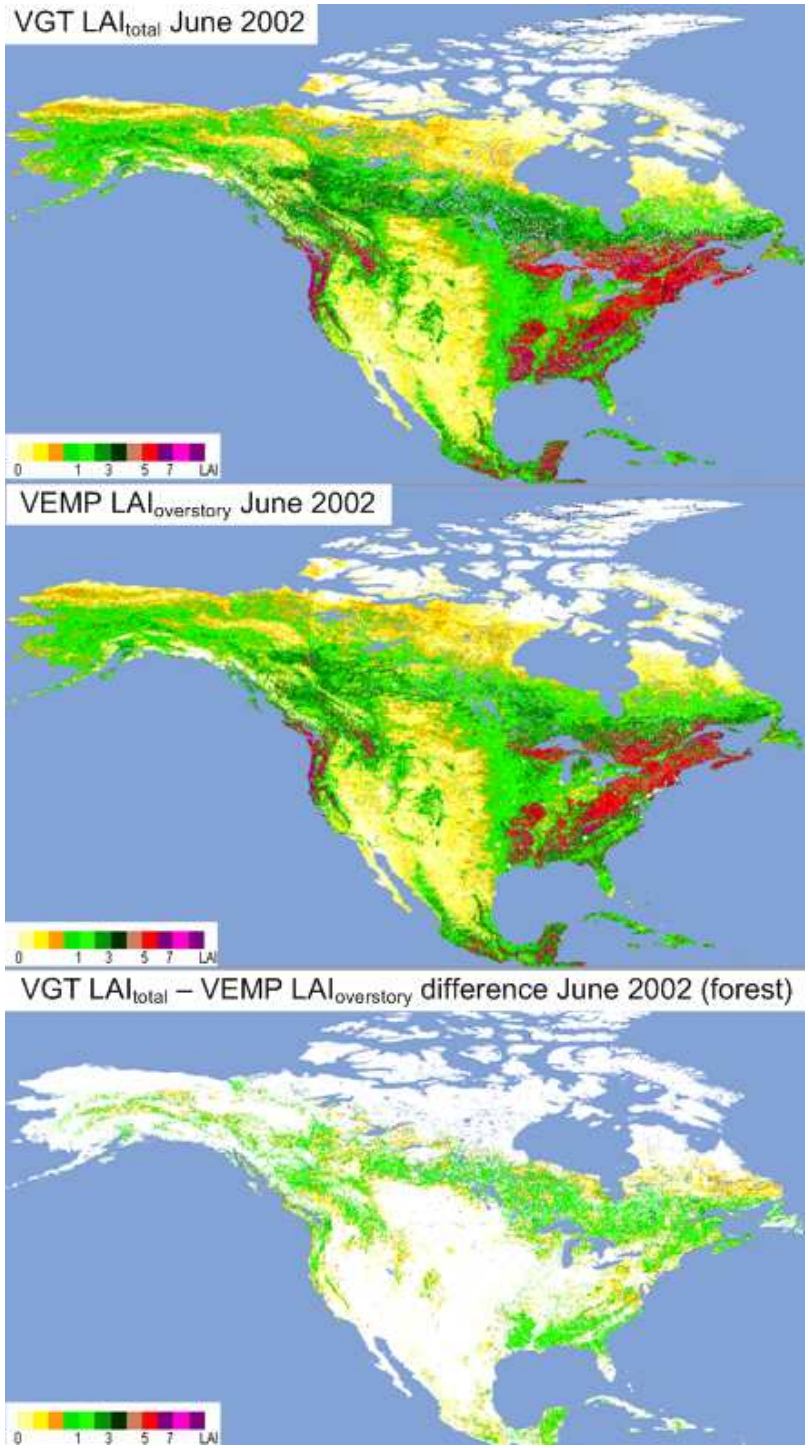

Pisek et al., 2010, JGR

Seasonal trajectories of VeMP vs. total LAI

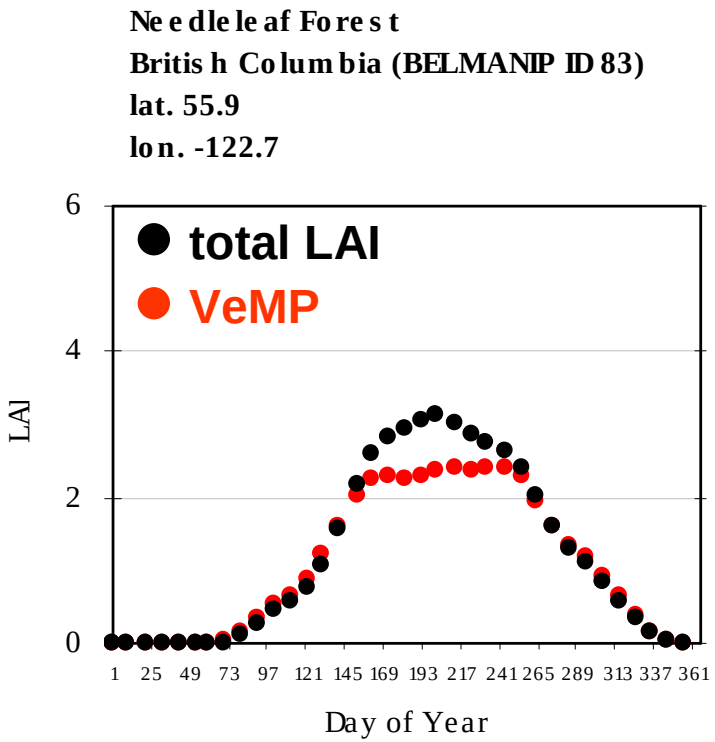

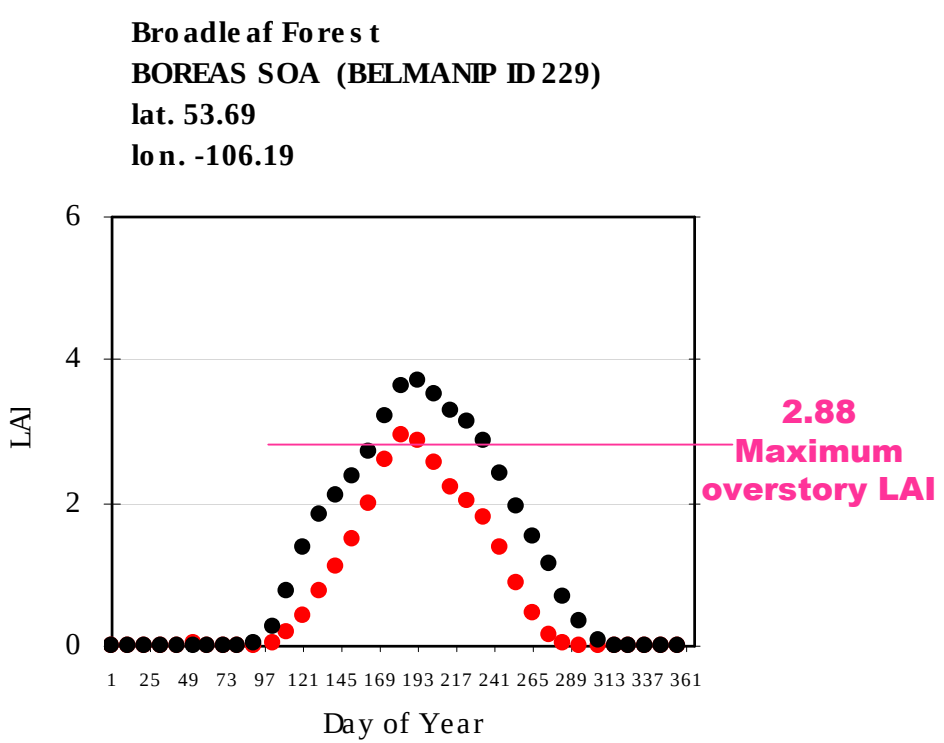

Pisek et al., 2010, JGR

VeMP LAI vs. MODIS Collection 5 LAI and BigFoot

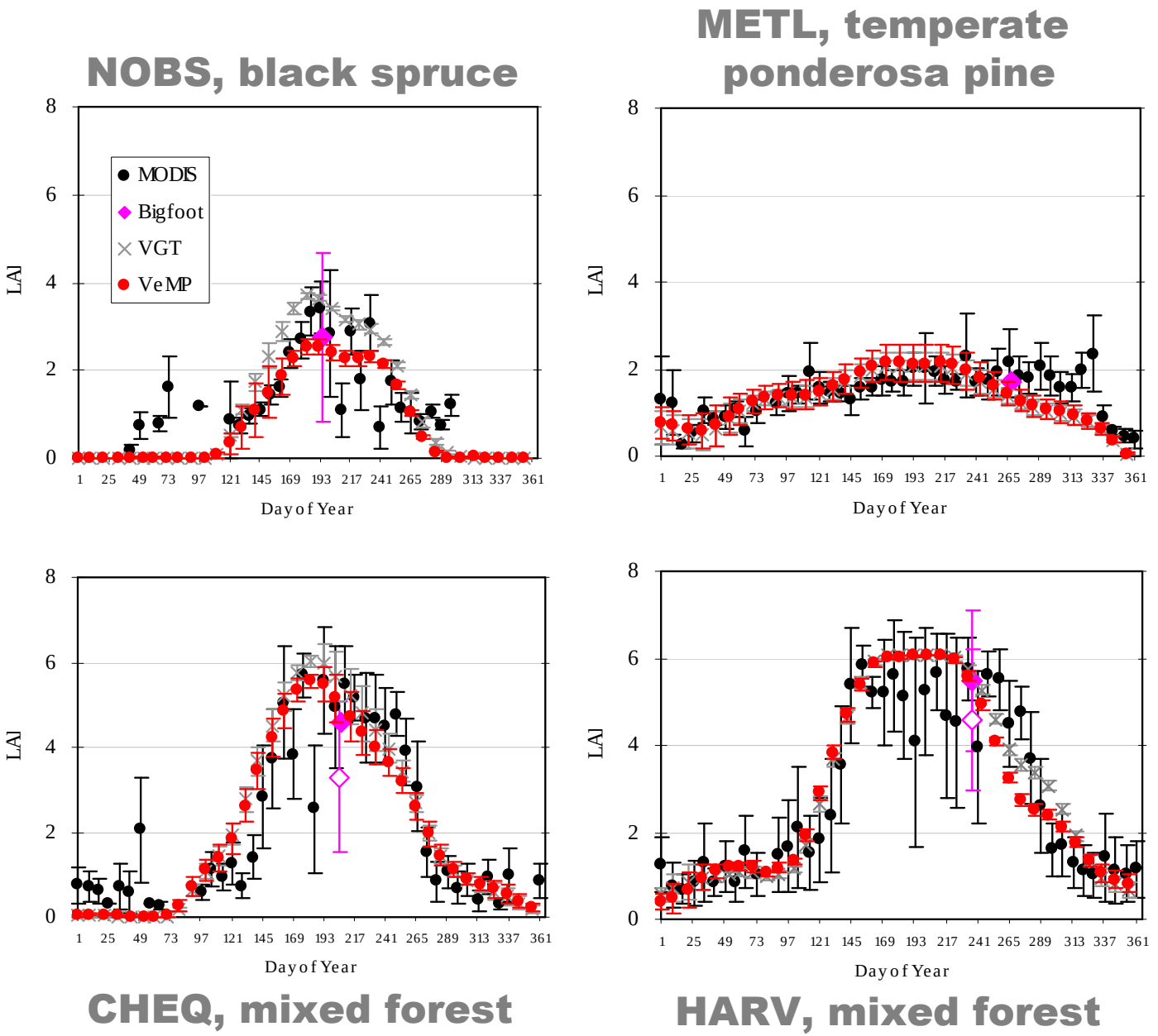

Pisek et al., 2010, JGR

Estimation of vegetation clumping index using MODIS BRDF data - Why?

- **POLDER clumping map too coarse at ~6km resolution**
- **Higher resolution maps desirable, especially since we already have the suitable sensors and models**

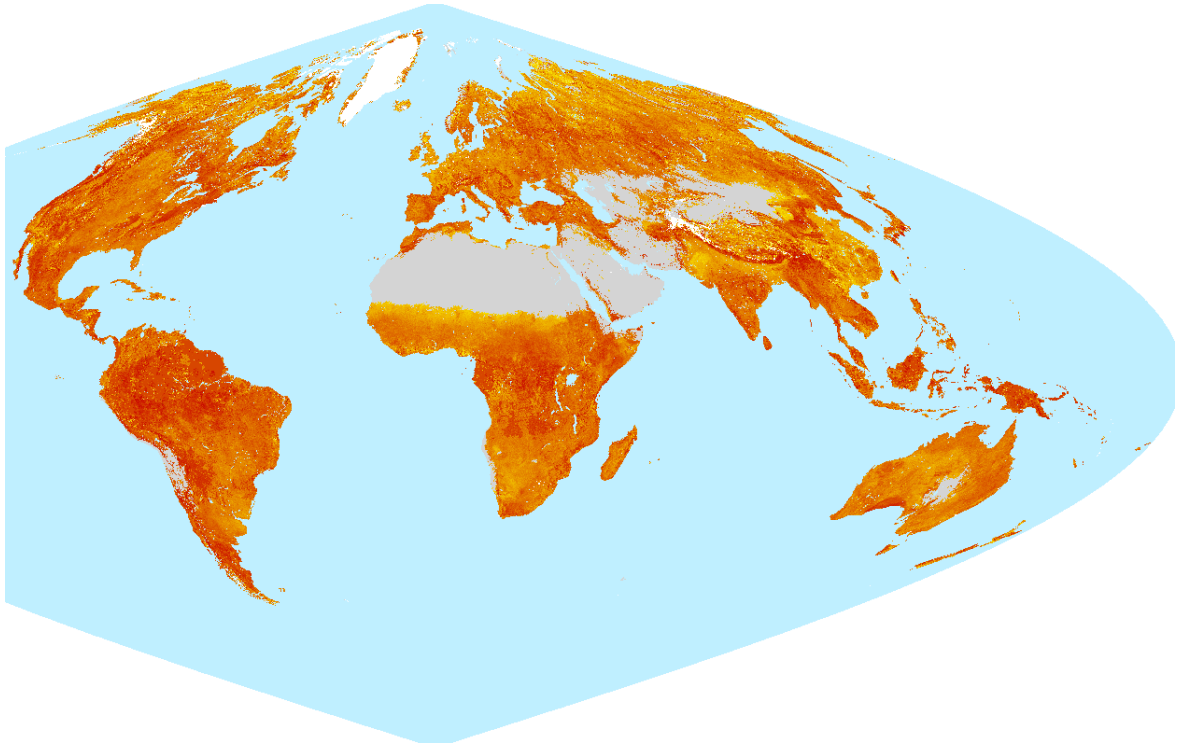

Clumping index from POLDER observations

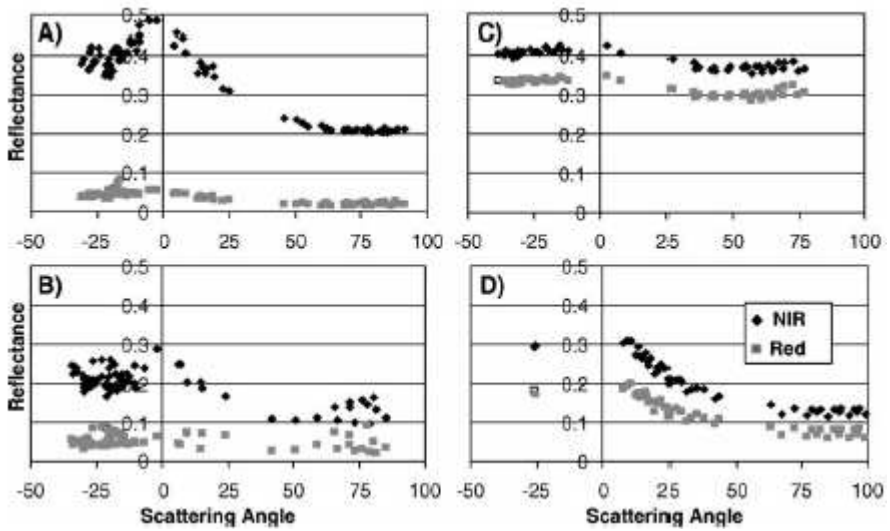

$$NDHD = (\rho_h - \rho_d)/(\rho_h + \rho_d)$$

$$\Omega = a(\mathrm{NDHD}) + b$$

Clumping index from MODIS BRDF parameters (every 16 days at 500m resolution)

MODIS BRDF parameters from MCD43A1.005 product

$$R(\theta_i,\theta_v,\Phi,\lambda) = f_{iso}(\lambda) + f_{vol}(\lambda)K_{vol}(\theta_i,\theta_v,\Phi) + f_{geo}(\lambda)K_{geo}(\theta_i,\theta_v,\Phi)$$

from Lucht et al. (2000, IEEE)

Check quality flags from MCD43A2.005

$$NDHD = (\rho_h - \rho_d)/(\rho_h + \rho_d)$$

$$\Omega = a(\mathrm{NDHD}) + b$$

Pisek et al., IJRS, in press

Sensitivity to the chosen geometry (+/-45d)

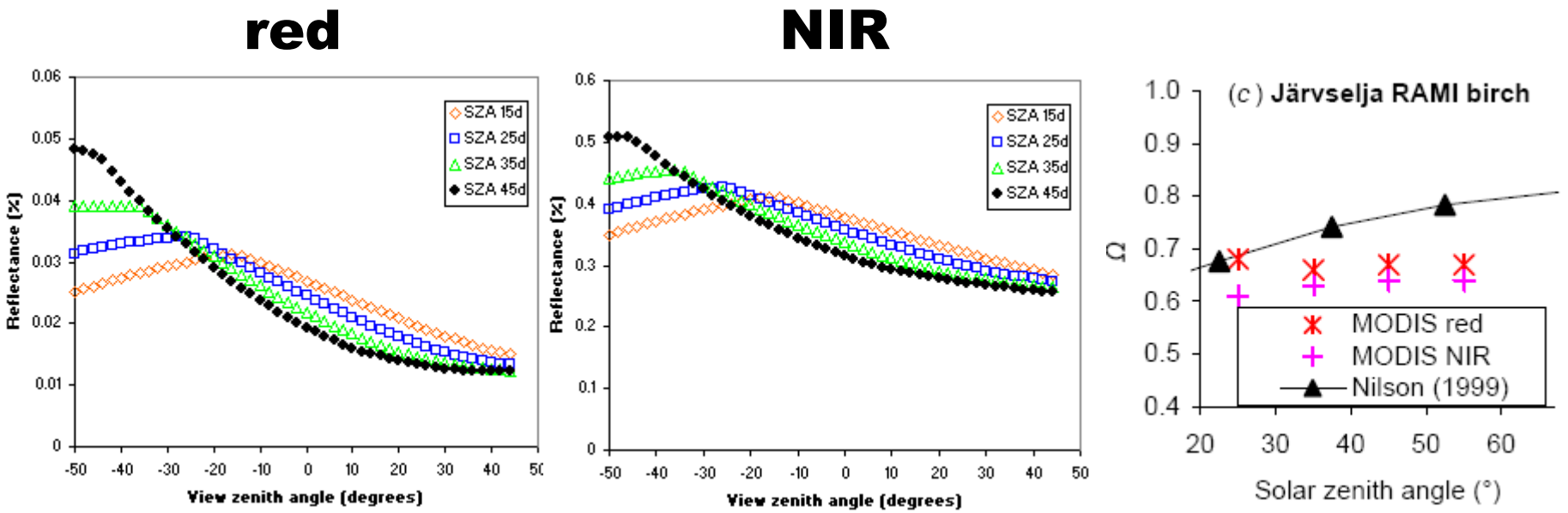

Pisek et al., IJRS, in press

Higher resolution has its advantages -validation dataset extended from 32 to 64 sites

ID	Site	Location
1	Mongu	Zambia
2	Pandametanga	Botswana
3	Maun	Botswana
4	Okwa River	Botswana
5	Tshane	Botswana
6	Heihe	China
7	Tonzi	USA
8	NOJP	Canada
9	SOJP	Canada
10	NYJP	Canada
11	SYJP	Canada
12	NOBS	Canada
13	SOBS	Canada
14a	Petawawa_a	Canada
14b	Petawawa_b	Canada
14	Petawawa	
15	Metolius	USA
16a	Kananaskis_a	Canada
16b	Kananaskis_b	Canada
16c	Kananaskis_c	Canada
16	Kananaskis	
17	F77	Canada
18	F98	Canada
19	SOJP	Canada
20	HJP75	Canada
21	HJP94	Canada
22	SOBS	Canada
23a	Mer Bleue	Canada
23b	Mer Bleue	Canada
23	Mer Bleue	
24	Sudbury	Canada
25	Takayama	Japan
26	Appomattox	USA
27	SETRES	USA
28	Hertford	USA
29	Black Hills	USA
30	Yatir	Israel
31a	Jarvselja_a	Estonia
31b	Jarvselja_b	Estonia
31c	Jarvselja_c	Estonia
31	Jarvselja	
32a	Bily Kriz_a	Czech Rep.
32b	Bily Kriz_b	Czech Rep.
32	Bily Kriz	

Location	Site
EBF	
Thailand	Kog-Ma
Kenya	Chaiwa
Kenya	Ngangao
DBF	
Netherlands	Millingerwaard_FR15
Netherlands	Millingerwaard_FR19
Sweden	Skarhult
Sweden	Fulltofta
Estonia	Järvselja RAMI birch
Russia	Krasnoyarsk K4
Russia	Krasnoyarsk K5
Japan	Takayama
Canada	SOA
Canada	NOA
Canada	Larose D1
Canada	Larose D2
ENF	
New Zealand	Okarito
Belgium	Pijnven
Czech Rep.	Bily Kriz_a
Czech Rep.	Bily Kriz_b
	Bily Kriz
Estonia	Järvselja RAMI spruce
Estonia	Järvselja RAMI pine
Russia	Krasnoyarsk K1
Russia	Krasnoyarsk K2
Israel	Yatir
USA	Appomattox
USA	SETRES
USA	Hertford
USA	Howland (Main)
USA	Howland (Block A)
USA	Black Hills
USA	Metolius

Canada	F98
Canada	SOJP
Canada	HJP75
Canada	HJP94
Canada	SOBS
Canada	EOBS
Canada	BF80
Canada	WPP74
Canada	IDF
Canada	F77
Canada	IBF
Canada	YBF
Canada	WPP89
Canada	WPP39
Canada	Kananaskis_a
Canada	Kananaskis_b
Canada	Kananaskis_c
	Kananaskis
Canada	Smooth Rock Falls
Canada	Sudbury
Canada	Petawawa_a
Canada	Petawawa_b
	Petawawa
Canada	NOJP
Canada	NYJP
Canada	SYJP
Canada	NOBS
Canada	SOBS
Canada	Larose P1
Canada	Larose P2
other	
Zambia	Mongu
Botswana	Pandametanga
Botswana	Okwa River
Botswana	Tshane
Botswana	Maun
China	Heihe
USA	Tonzi
Canada	Mer Bleue
Canada	Mer Bleue
	Mer Bleue

Pisek et al., IJRS, in press

MODIS clumping retrievals vs. field observations

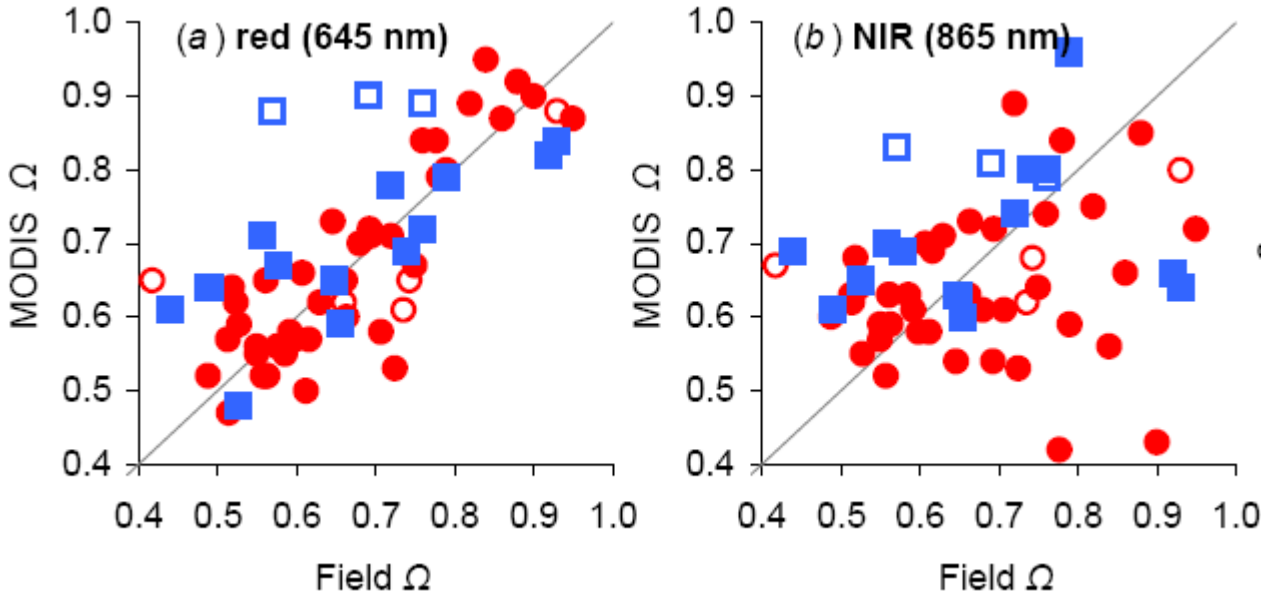

after 2002
- **best quality**
- **lower quality**

before 2002
- **best quality**
- **lower quality**

Pisek et al., IJRS, in press

Let’s not throw MODIS NIR results into garbage yet!

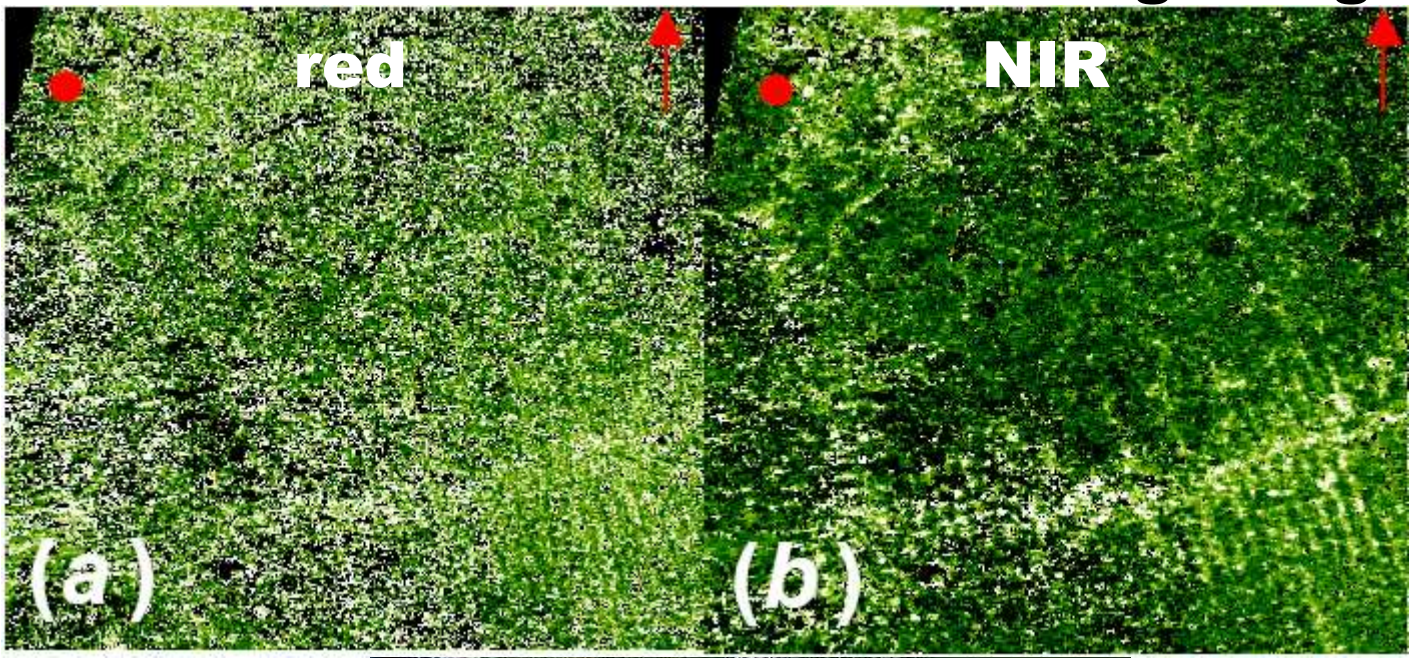

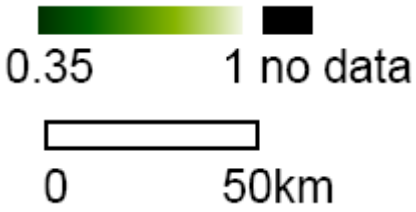

Pisek et al., IJRS, in press

How to determine what band to use?

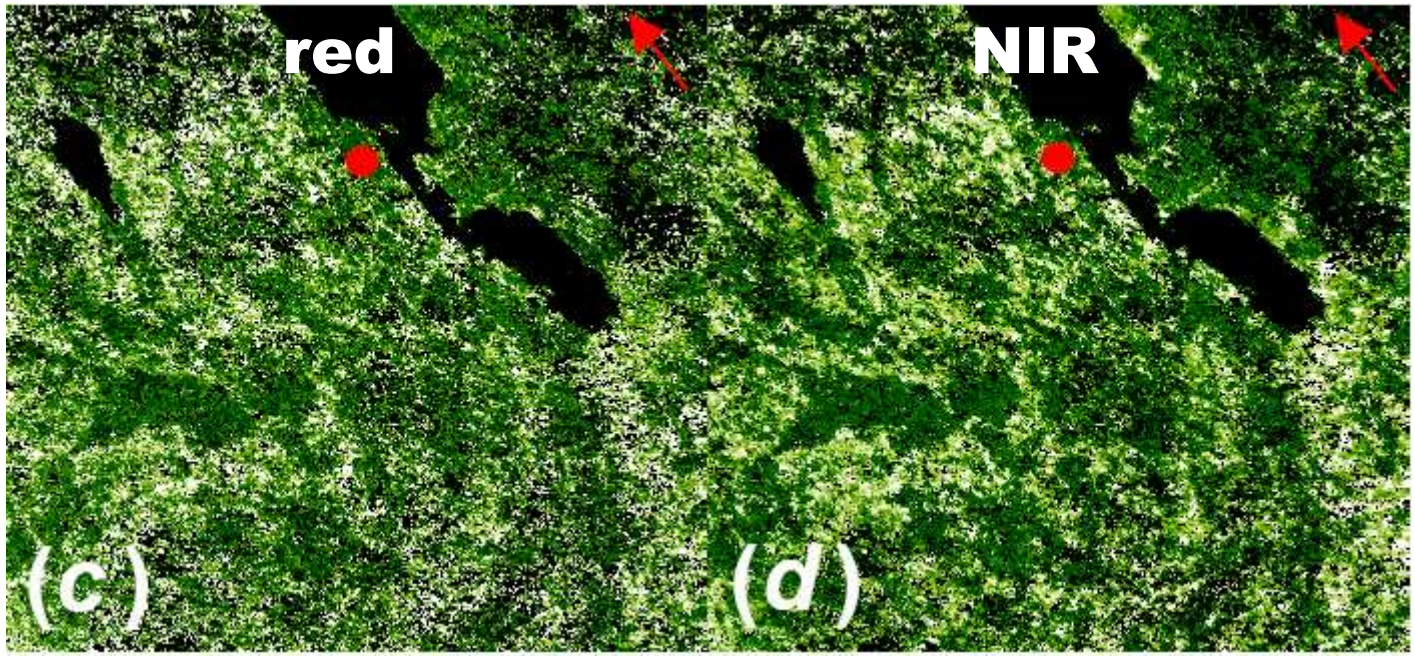

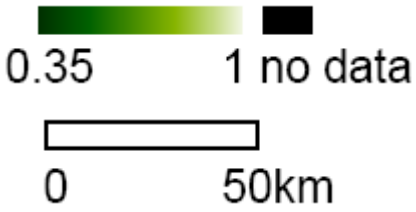

Pisek et al., IJRS, in press

The latest hot stuff from Tartu Observatory!

- A theoretical model for determining the required amount of LAI-2000 or digital hemispheric image measurements in a stand to ensure the desired accuracy of the leaf area index value derived from optical analyzer measurements by inversion of gap fraction data
- Nilson, T., Kuusk, A., Lang, M., Pisek, J., Kodar. A., 2011. Simulation of statistical characteristics of gap distribution in forest stands. Agricultural and Forest Meteorology.
- Model available upon request from: nilson@aai.ee